Calhoun: The NPS Institutional Archive
DSpace Repository

Theses and Dissertations 1. Thesis and Dissertation Collection, all items

1949

An analytical and experimental analysis of a linear damping dynamic vibration absorber

Ryder, Henry Shorb

Annapolis, Maryland. U.S. Naval Postgraduate School

http://hdl.handle.net/10945/31648

This publication is a work of the U.S. Government as defined in Title 17, United States Code, Section 101. Copyright protection is not available for this work in the United States.

Downloaded from NPS Archive: Calhoun

Calhoun is the Naval Postgraduate School's public access digital repository for research materials and institutional publications created by the NPS community. Calhoun is named for Professor of Mathematics Guy K. Calhoun, NPS's first appointed -- and published -- scholarly author.

Dudley Knox Library / Naval Postgraduate School
411 Dyer Road / 1 University Circle
Monterey, California USA 93943

http://www.nps.edu/library

AN ANALYTICAL AND EXPERIMENTAL ANALYSIS OF A LINEAR DAMPED DYNAMIC VIBRATION ABSORBER

H. S. RYDER

Library
U. S. Naval Postgraduate School
Annapolis, Md.

AN ANALYTICAL AND EXPERIMENTAL ANALYSIS
OF
A LINEAR DAMPED DYNAMIC VIBRATION ABSORBER

by

Henry S. Ryder
Lieutenant Commander, United States Navy

Submitted in partial fulfillment
of the requirements
for the degree of
MASTER OF SCIENCE
IN
MECHANICAL ENGINEERING

United States Naval Postgraduate School
Annapolis, Maryland
1949

This work is accepted as fulfilling

the thesis requirements for the degree of

MASTER OF SCIENCE
IN
MECHANICAL ENGINEERING

from the

United States Naval Postgraduate School

[redacted]

Chairman

Department of Mechanical Engineering

Approved:

[redacted]

Academic Dean , acting

11325

PREFACE

The theory of the damped dynamic vibration absorber, neglecting the effect of damping in the main mass system, has been worked out and is available in the literature. However, a search of the literature reveals a lack of experimental verification of the theory. This is probably due to the general unavailability of suitable experimental apparatus such as the Westinghouse vibration fatigue testing equipment recently acquired by the United States Naval Postgraduate School, and which is one of the first commercial units of this type to be built.

During the period from October 1948 through April 1949 the author extended the theory of the damped dynamic vibration absorber to include the effect of damping in the main mass system, designed a suitable absorber unit for application to an elastic system driven by the above noted fatigue testing equipment, and ran tests to obtain experimental verification of the theory. This work was carried on at the United States Naval Postgraduate School.

The author gratefully acknowledges the assistance and guidance rendered by Dr. Ernest K. Gatcombe of the U. S. Naval Postgraduate School during the entire project. Acknowledgements are also due to the U. S. Naval Engineering Experiment Station for the manufacture of the absorber unit, the furnishing of oil samples with viscosity data, and the photographic services rendered in the development and printing of oscillograms; to the Public Works Division of the U. S. Naval Academy for making tracings and prints; to Professor P. E. Cooper of the Postgraduate School for his assistance in the solution of certain electronic problems; to Mr. J. A. Oktavec of the mechanical force of the Postgraduate School for his fine workmanship in the manufacture of necessary experimental apparatus; and to various members of the staff and faculty in the Departments of Physics, Mechanical Engineering, Electrical Engineering, and Electronics Engineering of the Postgraduate School for the loan of instruments and apparatus.

TABLE OF CONTENTS

Page

PREFACE ii

LIST OF ILLUSTRATIONS AND TABLES vi

TABLE OF SYMBOLS viii

CHAPTER I. INTRODUCTION 1

CHAPTER II. MATHEMATICAL ANALYSIS 2 - 11

1. The Problem 2
2. Differential Equations of Motion 3
3. Steady State Solution 4
4. Dimensionless Form 5
5. Special Cases 6
6. Analysis of Solution 6
7. Other Considerations 10

CHAPTER III. APPARATUS 12 - 21

1. Purpose 12
2. The Absorber 12
3. The Mounting 12
4. The Vibration Motor 14
5. The Elastic System 14
6. The Vibration Equipment 16
7. Oscillographs 18
8. Amplitude Measuring Apparatus 19

CHAPTER IV. PROCEDURE AND RESULTS 22 - 50

1. Preliminary Considerations 22
2. Main System Spring Constant 22

3. Absorber System Spring Constant 22
4. Mass of Absorber System 26
5. Natural Frequency of Absorber System 29
6. Mass of Main System 29
7. Summary of System Constants 30
8. Amplitude Response Tests 31
9. Theoretical Curves 34
10. Absorber Temperature Rise 44
11. Main System Damping Constant 45
12. Oscillograms 45
CHAPTER V. DISCUSSION AND CONCLUSIONS 51 - 54
BIBLIOGRAPHY 55

LIST OF ILLUSTRATIONS AND TABLES

		Page
Fig. 1.	Diagram of Elastic System	2
Fig. 2.	Absorber Mounting Details	13
Fig. 3.	Motor Assembly	15
Fig. 4.	Simplified Schematic Diagram, 40 Watt System	17
Fig. 5.	Overall View of Apparatus	20
Fig. 6.	Close-up of Vibration Motor	20
Fig. 7.	Temperature Measuring Apparatus	21
Fig. 8.	Method of Static Loading for Determination of Main Spring Constant	23
Fig. 9.	Measurement of Static Deflection for Determination of Main Spring Constant	23
TABLE I.	Experimental Data for Determination of Main System Spring Constant	24
Fig. 10.	Curve for Spring Constant of Main System	25
Fig. 11.	Jig for Measuring Absorber System Spring Constant	26
TABLE II.	Experimental Data for Determination of Absorber System Spring Constant	27
Fig. 12.	Curve for Spring Constant of Absorber System	28
Fig. 13.	Oil Viscosity Curves	33
TABLE III.	Experimental Data for Determination of Static Displacement of Main System	35
Fig. 14.	Determination of Static Displacement of Main System	36
TABLE IV.	Experimental Data for Case of Constant Tuning	37
TABLE V.	Computed Points for Plotting Theoretical Curve for Case of Constant Tuning and Infinite Damping	38
Fig. 15.	Curves for Constant Tuning	39
TABLE VI.	Experimental Data for Case of Optimum Tuning	40

TABLE VII. Computed Points for Plotting Theoretical Curve for Case of Optimum Tuning and Infinite Damping 41

TABLE VIII. Computed Points for Plotting Theoretical Curves for Case of Optimum Tuning 42

Fig. 16. Curves for Optimum Tuning 43

TABLE IX Experimental Data for Absorber Temperature Rise Curves 46

Fig. 17. Absorber Temperature Rise Curves 47

Fig. 18. Oscillogram of Die-Away Characteristic of Main System for Determination of Damping Constant 48

Fig. 19. Oscillogram Showing Effect of Absorber on Die-Away Characteristic Using Navy Symbol No. 3042 Oil 49

Fig. 20. Oscillogram Showing Effect of Absorber on Die-Away Characteristic Using Navy Symbol No. 2135 Oil 49

Fig. 21. Oscillogram Showing Effect of Absorber on Die-Away Characteristic Using Navy Symbol No. 1065 Oil 50

Fig. I. Detail Plan of Damped Dynamic Absorber (Back Cover)

TABLE OF SYMBOLS

b	Main system damping constant
b_c	Critical damping constant of main system $= 2M\Omega_n$.
c	Absorber system damping constant
c_c	(Pseudo) Critical damping constant of absorber system $= 2m\Omega_n$.
d	Wire diameter of absorber spring in inches
f	Tuning ratio $= \omega_a/\Omega_n$
f_1	Natural frequency of one absorber spring in cycles per sec.
g	Driving frequency ratio $= \omega/\Omega_n$
h	Damping ratio $= c/c_c$
j	Complex operator $\sqrt{-1}$
K	Main system spring constant
k	Absorber system spring constant
k_s	Spring constant of one absorber spring
M	Mass of main system
m	Mass of absorber system
m_s	Mass of one absorber spring
n	Number of active turns of one absorber spring
P_o	Maximum value of exciting force
Q	Damped natural frequency of main system
r	Mean radius of absorber spring in inches
t	Time
x_1	Displacement of main mass from neutral position
x_2	Displacement of absorber mass from neutral position
x_o	Static deflection of main system $= P_o/K$
d/dt	First derivative with respect to time
d^2/dt^2	Second derivative with respect to time

ϵ	Natural logarithm base
μ	Mass ratio $= m/M$
Ω_n	Undamped natural frequency of main system* $= \sqrt{K/M}$
ω	Driving frequency*
ω_a	Undamped natural frequency of absorber system* $= k/m$
ω_n	Natural frequency of one absorber spring
∞	Infinity

---

*ω, ω_a, and Ω_n are circular frequencies in radians per sec. unless specifically designated as cycles per second, in which case multiply by 2π to obtain radians per sec.

CHAPTER I

INTRODUCTION

When an elastic system is acted upon by a steady alternating force of constant frequency, it may develope obnoxious vibrations, especially when the frequency of the force is close to the resonant frequency of the elastic system. Such resonant phenomenon is frequently encountered in machines and machine members when operating close to a critical speed or during acceleration through a critical speed. In order to eliminate or reduce the objectionable vibration, several possibilities should be investigated. The elimination or reduction of the exciting force would be the ideal solution, but this may not be practicable or even possible. The mass or the spring constant of the system might be changed in order to get away from the resonant condition, but this may also be impractical. A third possibility is the application of a dynamic vibration absorber.

This investigation is concerened with the development of the mathematical theory of a linear damped vibration absorber and the correlation of this theory with experimental results obtained from the application of an absorber to a vibrating system.

CHAPTER II

MATHEMATICAL ANALYSIS

1. The Problem.-

Consider the damped two-degree-of-freedom system represented diagrammatically in Fig. 1. Let the combination K,M represent the elastic system of the machine or member which is vibrating under the influence of a sinusoidal force, $P_o \mathrm{Sin}\, \omega t$. This system will subsequently be refered to as the main system. Attached to the main mass is a small elastic system, k,m, which represents the dynamic absorber; this system will subsequently be refered to as the absorber system. Both masses are assumed to be guided so as to be capable of purely vertical motions only. A viscous damper, represented by a dashpot, with a damping constant b, is attached between the main mass, M, and the rigid support, A, and represents the damping which is present in all physical elastic systems, although it may be quite small. Another viscous damper, with damping constant, c, is attached between the absorber mass and the main mass, and represents damping deliberately introduced in the absorber system as well as the natural damping which exists in the system. For simplification of the analysis, the assumption is made that only viscous type damping is present in the two systems. The positive direction is taken as downward with the neutral, or equilibrium, position of each mass system as indicated in the figure.

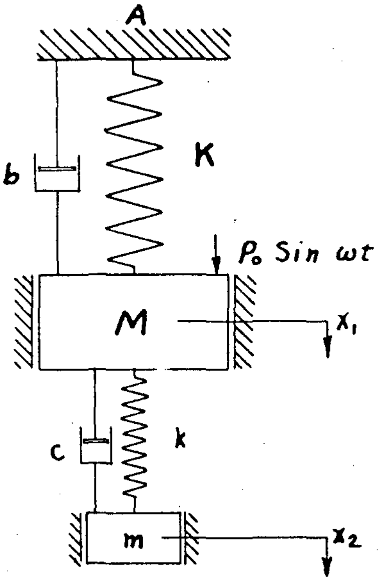

Fig. 1

The problem is to calculate the steady-state forced vibration of the main mass under the influence of the sinusoidal exciting force and the absorber action.

2. Differential Equations of Motion.-

Consider the instant when the main mass, M, is being displaced downward, in the positive direction, from the equilibrium position. The forces acting on the main mass, M, are:

Main spring force,	$-Kx_1$
Absorber spring force,	$-k(x_1 - x_2)$
Main system damping force,	$-b(dx_1/dt)$
Absorber system damping force,	$-c(dx_1/dt - dx_2/dt)$
Impressed exciting force,	$+P_0 \mathrm{Sin}\, \omega t$

The forces acting on the absorber mass, m, are:

Absorber spring force,	$+k(x_1 - x_2)$
Absorber damping force,	$+c(dx_1/dt - dx_2/dt)$

By the application of Newton's second law (Force = Mass x Acceleration) to each mass, and arrangement of terms, the equations of motion for the two-degree-of-freedom system may be written:

$$M\frac{d^2x_1}{dt^2} + Kx_1 + k(x_1 - x_2) + b\frac{dx_1}{dt} + c\left(\frac{dx_1}{dt} - \frac{dx_2}{dt}\right) = P_0 \,\mathrm{Sin}\,\omega t \tag{1}$$

$$m\frac{d^2x_2}{dt^2} + k(x_2 - x_1) + c\left(\frac{dx_2}{dt} - \frac{dx_1}{dt}\right) = 0 \tag{2}$$

3. Steady State Solution.-

For the steady-state solution, both x_1 and x_2 are harmonic motions of the frequency ω and can be represented by rotating vectors. Also, each term in equations (1) and (2) is representable by such a vector rotating at velocity ω. Equations (1) and (2) may be expressed as complex numbers as follows:

$$\left[-M\omega^2 + K + k + j\omega(b+c)\right] x_1 - \left[k + j\omega c\right] x_2 = P_0 \tag{3}$$

$$-\left[k + j\omega c\right] x_1 + \left[-m\omega^2 + k + j\omega c\right] x_2 = 0 \tag{4}$$

where x_1 and x_2 are (unknown) complex numbers and the other quanties are real. Solving equation (4) for x_2, substituting this in equation (3) and solving for x_1, there results:

$$\frac{x_1}{P_0} = \frac{(k - m\omega^2) + j\omega c}{\left[(-M\omega^2+K)(-m\omega^2+k) - m\omega^2 k - \omega^2 bc\right] + j\omega c\left[-M\omega^2+K-m\omega^2+\frac{b}{c}(-m\omega^2+k)\right]} \tag{5}$$

This is of the form

$$\frac{x_1}{P_0} = \frac{A + jB}{C + jD} \tag{6}$$

which, by the simple application of the rules of complex numbers, has an absolute value of the form

$$\left|\frac{x_1}{P_0}\right| = \sqrt{\frac{A^2 + B^2}{C^2 + D^2}} \tag{7}$$

By applying this form to equation (5) there results:

$$\left|\frac{X_1}{P_o}\right| = \sqrt{\frac{(k-m\omega^2)^2 + \omega^2 c^2}{\left[(-M\omega^2+K)(-m\omega^2+k) - m\omega^2 k - \omega^2 bc\right]^2 + \omega^2 c^2\left[-M\omega^2+K-m\omega^2+\frac{b}{c}(-m\omega^2+k)\right]^2}} \qquad (8)$$

4. Dimensionless Form.-

Equation (8) may be used to calculate the amplitude of vibration, which is a function of eight variables: P_o, ω, b, c, K, k, M, and m. However, in order to reduce the number of variables and to better demonstrate the physical factors involved, it is desirable to write equation (8) in dimensionless form, utilizing the following symbols:

μ = m/M = mass ratio.

$\omega_a = \sqrt{k/m}$ = undamped natural (circular) frequency of absorber.

$\Omega_n = \sqrt{K/M}$ = Undamped natural frequency of main system.

f = $\frac{\omega_a}{\Omega_n}$ = tuning ratio.

g = $\frac{\omega}{\Omega_n}$ = driving frequency ratio.

$x_o = P_o/K$ = static deflection of main system.

$\frac{X_1}{X_o}$ = amplitude ratio of main system.

$c_c = 2m\Omega_n$ = (pseudo) critical damping constant.

h = c/c_c = damping ratio.

By dividing both the numerator and denomenator of equation (8) by $c_c^2\Omega_n^2$, making appropriate substitutions from the above listed dimensionless parameters, and with simple algebraic ~~manuplication~~ manipulation, there results:

$$\left|\frac{X_1}{X_o}\right| = \sqrt{\frac{(2hg)^2 + (g^2-f^2)^2}{(2hg)^2\left[g^2-1+\mu g^2 \underset{\uparrow}{+} \mu\frac{b}{c_o}(g^2-f^2)\right]^2 + \left[\mu f^2 g^2 - (g^2-1)(g^2-f^2) + 4\mu h g^2\frac{b}{c_c}\right]^2}} \qquad (9)$$

For any given system operating under specified conditions, the dimensionless quanties h, b/c_c, b/c, f, and μ, may be considered as constants, and the frequency ratio, g, as the independent variable. The amplitude ratio x_1/x_o of the main mass is, then, a function of g only.

5. Special Cases.-

It is interesting to investigate equation (9) for certain special cases. When the damping, c, of the absorber system approaches zero, h approaches zero, and equation (9) reduces to

$$\left|\frac{x_1}{x_0}\right| = \sqrt{\frac{(g^2 - f^2)^2}{\left[2\mu g \frac{b}{C_c}(g^2 - f^2)\right]^2 + \left[\mu f^2 g^2 - (g^2 - 1)(g^2 - f^2)\right]^2}} \tag{10}$$

It will be noted that the amplitude ratio becomes zero when $g = f$. However, if b is small a high resonant peak will occure on each side of f, and these peaks will approach infinity as b approaches zero.

When c of equation (9) approaches infinity, the absorber mass is, in effect, locked to the main mass and the vibrating system becomes a single-degree-of-freedom system with a mass (M + m). For this case, equation (9) may be simplified by dividing the numerator and deminator by $(2hg)^2$, and letting c approach infinity, giving

$$\left|\frac{x_1}{x_0}\right| = \sqrt{\frac{1}{\left[g^2 - 1 + \mu g^2\right]^2 + \left[2\mu g \frac{b}{C_c}\right]^2}} \tag{11}$$

which has a resonant peak when $g = \sqrt{\frac{1}{1+\mu}}$ and this peak will approach infinity as b approaches zero.

6. Analysis of Solution.-

Equation (9) may be shown to be of the form

$$\left|\frac{x_1}{x_0}\right| = \sqrt{\frac{Ah^2 + B}{Ch^2 + Eh + D}} \tag{12}$$

where:

$$
\begin{aligned}
A &= 4g^2 \\
B &= (g^2 - f^2)^2 \\
C &= 4g^2(g^2 - 1 + \mu g^2)^2 + \left(4\mu g \tfrac{b}{c_c}\right)^2 \\
E &= 8\mu g^2(g^2 - 1 + \mu g^2)(g^2 - f^2)\frac{b}{c_c} - 8\mu g^2\left[\mu f^2 g^2 - (g^2 - 1)(g^2 - f^2)\right]\frac{b}{c_c} \\
D &= 4\mu^2 g^2(g^2 - f^2)^2\left(\frac{b}{c_c}\right)^2 + \left[\mu f^2 g^2 - (g^2 - 1)(g^2 - f^2)\right]^2
\end{aligned}
\tag{13}
$$

There is no relationship amoung the terms A, B, C, D, E, which will make equation (12) independent of the damping ratio, h, unless $g = 0$, which is a trivial case, or $b = 0$, in which case equation (12) reduces to

$$\left|\frac{x_1}{x_0}\right| = \sqrt{\frac{Ah^2 + B}{Ch^2 + D}} \tag{14}$$

and all terms in (13) containing b becomes zero. Equation (14) is independent of damping if

$$\frac{A}{C} = \frac{B}{D} \tag{15}$$

When b is zero, equation (9) reduces to the special case treated by Den Hartog (3), and may be written:

$$\left|\frac{x_1}{x_0}\right| = \sqrt{\frac{(2hg)^2 + (g^2-f^2)^2}{(2hg)^2(g^2-1+\mu g^2)^2 + \left[\mu f^2 g^2 - (g^2-1)(g^2-f^2)\right]^2}} \tag{16}$$

It is recommended that the interested reader refer to this text for the details of mathematical development which, in general, are omitted in the interest of brevity in the analysis which follows.

Substituting relations from (13) in (15), for the case of $b = 0$, there results,

$$\left[\frac{1}{g^2-1+\mu g^2}\right]^2 = \left[\frac{(g^2-f^2)}{\mu f^2 g^2 - (g^2-1)(g^2-f^2)}\right]^2 \tag{17}$$

from which,

$$\mu f^2 g^2 - (g^2-1)(g^2-f^2) = \pm (g^2-f^2)(g^2-1+\mu g^2) \tag{18}$$

For the case of the minus sign, equation (18) reduces to

$$\mu f^2 g^2 = -\mu g^2 (g^2-f^2)$$

from which it is seen that $g = 0$, which is proof of the obvious fact that at zero frequency, the amplitude ratio is independent of damping. An inspection of equation (16) also shows that at zero frequency $x_1/x_o = 1$, or the deflection of the main mass is equal to the static deflection caused by P_o.

For the case of the plus sign, equation (18) reduces to

$$g^4 - 2g^2 \frac{1+f^2+\mu f^2}{2+\mu} + \frac{2f^2}{2+\mu} = 0 \tag{19}$$

which will have two roots, g_1^2 and g_2^2, the abscissas of the points (refered to as points P and Q in the literature) through which all curves on the $(g, x_1/x_o)$ plane will pass for any given value of f.

For the case of constant tuning, $f = 1$, the abscissas of points P and Q are respectively,

$$g_1 = \sqrt{1 - \sqrt{\frac{\mu}{2+\mu}}} \quad ; \quad g_2 = \sqrt{1 + \sqrt{\frac{\mu}{2+\mu}}} \tag{20}$$

while the ordinates are, respectively,

$$\left(\frac{x_1}{x_0}\right)_{q=q_1} = \frac{1}{(1+\mu)\sqrt{\frac{\mu}{(2+\mu)}} - \mu}$$

$$\left(\frac{x_1}{x_0}\right)_{q=q_2} = \frac{1}{(1+\mu)\sqrt{\frac{\mu}{(2+\mu)}} + \mu} \tag{21}$$

It will be noted that the ordinate of point P is greater than that of Q. Optimum damping will occure for the curve with a horizontal tangent through the point P. Brock (1) shows that this occures when

$$h^2 = \frac{\mu(3+\mu)\left[1+\sqrt{\frac{\mu}{2+\mu}}\,\right]}{8(1+\mu)} \tag{22}$$

from which the optimum damping constant may be computed, since $h = c/c_c$ and $c_c = 2m\,\Omega_n$.

Den Hartog (3) shows that by adjusting the tuning f, the ordinate of point P may be decreased and the ordinate of point Q increased until they are of equal magnitude, and the most optimum tuning is thereby effected. This occures when

$$f = \frac{1}{1+\mu} \tag{23}$$

It is evident from equation (23), since $f = \omega_a/\Omega_n$, that for optimum tuning the undamped natural frequency of the absorber should be somewhat lower than the undamped natural frequency of the main system. For example, an absorber 1/20 as large as the main system should have ω_a tuned 4.8% lower than Ω_n; and for an absorber 1/10 as large, ω_a should be 9.1% lower.

For the case of optimum tuning, the abscissas of points P and Q of the $(g, x_1/x_0)$ diagram are respectively,

$$g_1 = \sqrt{\frac{1 - \sqrt{\frac{\mu}{2+\mu}}}{1+\mu}} \quad ; \qquad g_2 = \sqrt{\frac{1 + \sqrt{\frac{\mu}{2+\mu}}}{1+\mu}} \tag{24}$$

while the common ordinate is

$$\left(\frac{x_1}{x_0}\right)_{g=g_1} = \left(\frac{x_1}{x_0}\right)_{g=g_2} = \sqrt{1 + \frac{2}{\mu}} \tag{25}$$

The damping ratio which will give a curve with a horizontal tangent at point P will not have a horizontal tangent at Q, and vice versa, although the difference between the two constants is small. Brock (1) shows that a good average damping constant is

$$h^2 = \frac{3\mu}{8(1+\mu)^3} \tag{26}$$

7. Other Considerations.-

In the development of equation (9), a (pseudo) critical damping constant was defined as, $c_c = 2m\Omega_n$. It would seem more logical to define $c_c = 2m\omega_a$. If this definition of c_c is used, equation (9) would be replaced by

$$\frac{x_1}{x_0} = \sqrt{\frac{(2hfg)^2 + (g^2 - f^2)^2}{(2hfg)^2\left[g^2 - 1 + \mu g^2 + \mu \frac{b}{c}(g^2 - f^2)\right]^2 + \left[\mu f^2 g^2 - (g^2-1)(g^2-f^2) + 4\mu f^2 g^2 h \frac{b}{c_c}\right]^2}} \tag{27}$$

which differs from equation (9) by having the term f appear as a multiplier of the terms h and b/c_c. For any given system operating under specified conditions, equations (9) and (27) would give identical numerical answers. In order to agree with existing literature on this subject, it was deemed advisable to continue using a (pseudo) critical damping constant defined as $c_c = 2m\,\Omega_n$.

The above analysis is based on a harmonic exciting force having an amplitude independent of its frequency. Brock (2) has worked out the case in which the amplitude of the harmonic exciting force varies as the square of its frequency. The reader is refered to the literature for this interesting and important variation.

CHAPTER III

APPARATUS

1. Purpose.-

In order to obtain experimental verification of the theory of Chapter II, a damped dynamic vibration absorber was applied to an elastic system excited by a vibration motor and measurements were taken of the amplitude of vibration over the critical frequency range for various conditions of operation.

2. The Absorber.-

A detailed plan of the absorber unit designed by the author is enclosed as Fig. I, attached to the back cover. It consists, essentially, of a steel cylinder ~~cylinder~~, 2-3/4" long, with an inside diameter of 1½", fitted with top and bottom cover plates. A close fitting steel plunger of light construction, 2¼" long, with an H-shaped longitudinal cross-section, is supported inside the cylinder by means of helical compression springs which bear against the top and bottom cover plates. An 1/8" steel rod is attached to the plunger and protrudes through the top cover so that small weights may be added to the plunger for tuning purposes. The plunger may be locked in place by means of a brass set screw in the top cover which tightens against a flat milled on the plunger rod. Viscous damping between the plunger and cylinder is obtained by an oil film in the radial clearance space, which by measurement was .0022" thick.

3. The Mounting.-

The absorber unit was mounted at mid span of a fixed-ended steel beam of approximate dimensions: 1/8" thick, 1½" wide, and 10½" between

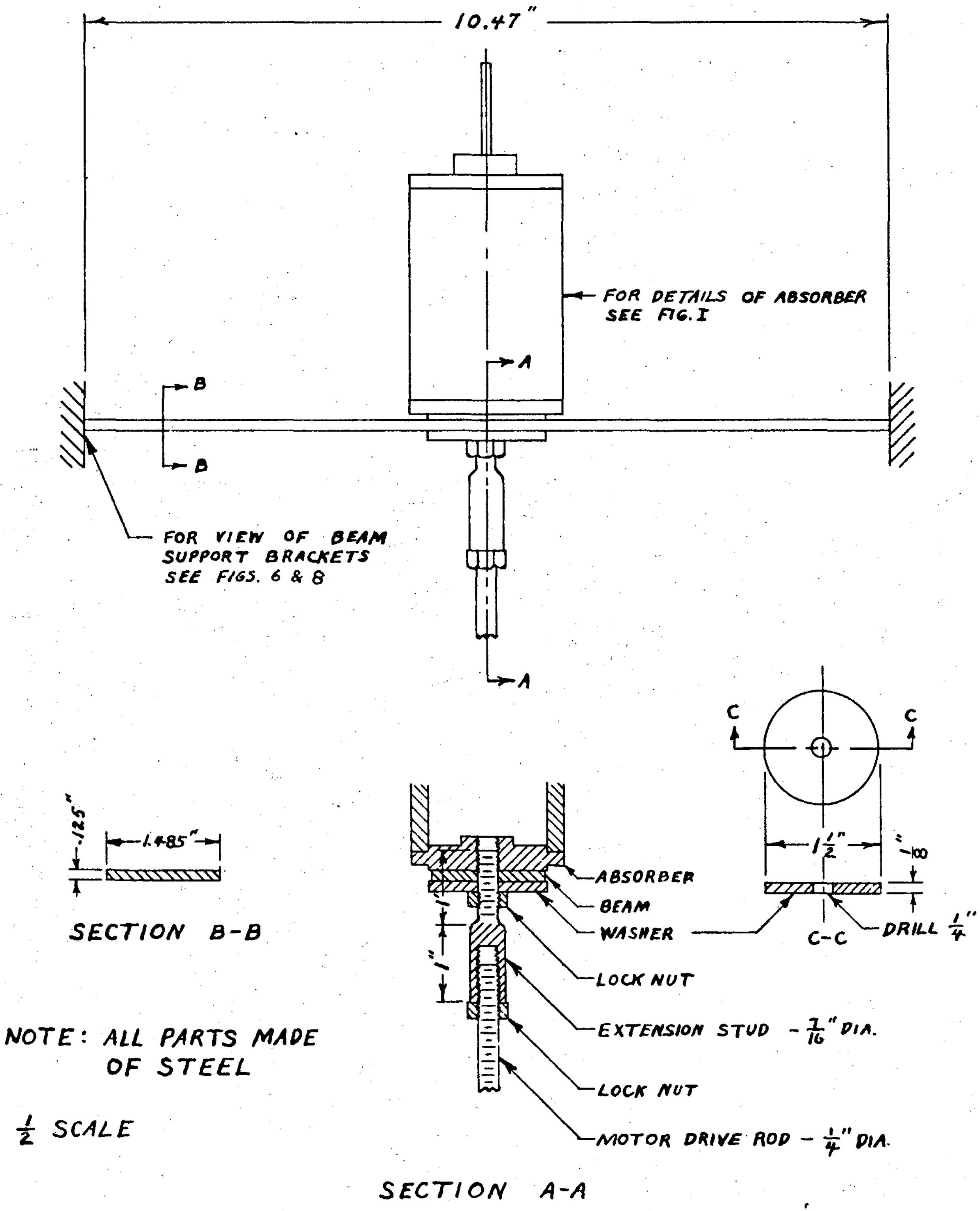
10.47"
FOR DETAILS OF ABSORBER SEE FIG. I
A
A
B
B
FOR VIEW OF BEAM SUPPORT BRACKETS SEE FIGS. 6 & 8
.125"
1.485"
SECTION B-B
C
C
1 1/2"
.100"
C-C
DRILL 1/4"
ABSORBER
BEAM
WASHER
LOCK NUT
EXTENSION STUD - 7/16" DIA.
LOCK NUT
MOTOR DRIVE ROD - 1/4" DIA.
1"
1"
SECTION A-A

NOTE: ALL PARTS MADE OF STEEL

1/2 SCALE

FIG. 2

ABSORBER MOUNTING DETAILS

supports. The exact dimensions and details of mounting and connection to the drive rod of the vibration motor are shown in Fig. 2.

4. The Vibration Motor.-

The vibration motor consists essentially of a coil placed in a uniform magnetic field. This coil is fastened rigidly, by means of a spider, to a drive rod which can be attached to any mechanical system. The spring suspension is such that the maximum amplitude of vibration is approximately 1/16" from the neutral position. A cut-away view of the motor assembly, as reproduced from the manufacturer's instruction manual, is shown in Fig. 3.

5. The Elastic System.-

By comparison of the above described elastic system with the diagrammatic system of Fig. 1, certain similarities are apparent. The combined spring constants of the fixed-ended beam and the spring suspension of the vibration motor drive coil assembly corresponds to K of Fig. 1. The mass of the motor drive coil assembly, inertia (effective) mass of the motor spring suspension, inertia (effective) mass of the fixed-ended beam, mass of the absorber mounting fittings (drive rod extension stud with lock nuts and the 1½" diameter steel washer on under side of beam), and entire mass of the absorber unit, excepting the plunger assembly, all add together and constitute M of Fig. 1. The combined spring constants of the two small helical compression springs in the absorber (the springs are in a parallel arrangement so that the spring constants add) corresponds to k. The mass of the plunger assembly (plunger with rod, two collars and four nuts) plus the inertia mass of the two springs, corresponds with the mass m of Fig. 1. The natural damping within the motor and beam

NOTE:-
PT 31 BUY FROM WILCOX CRITTENDON & CO. MIDDLETOWN CONN. CAT FIG 120½ 13"X8" GALVANIZED, WITH NUTS.
PTS. 2, 3, 20 - FIN PT 20 135A, THEN
CLEAN ALL THREE PTS. WITH LACQUER THINNER M-2525,
ASSEMBLE & FIN. 189-B — DO NOT GET PAINT IN
VIBRATOR OPENING - PAINT ALL OTHER SURFACES

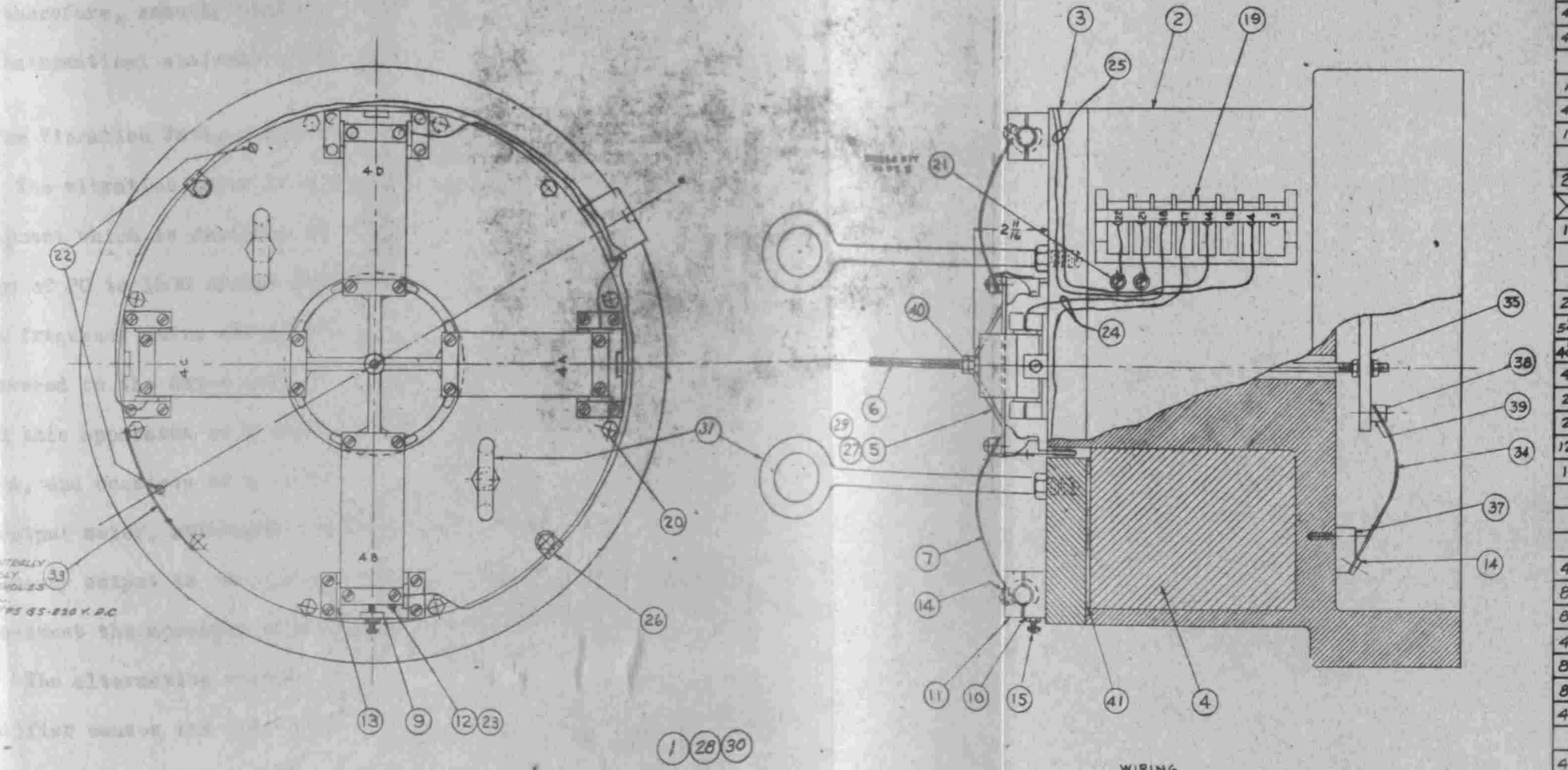

WIRING
CONNECT 4A TO 18V ON TERM. BLOCK.
CONNECT 4B TO 17V ON TERM. BLOCK.
CONNECT 4C TO 14V ON TERM. BLOCK.
CONNECT 4D TO 4V ON TERM. BLOCK.

G-3	G-2	G-1		NAVY TYPE NO.	MATERIAL	REFERENCE	PART	DESCRIPTION	FIN.
1	1	1			MICARTA #444		41	SPACER-COIL-14⅞ OD X 5 11/16 I.D. OF ⅛ TK	
2	2	2			BRASS		40	NUT(HEX) ¼-20	2-D
4	4	4				PT.3 7407129	39	BLOCK	
4	4	4				PT.2 7407129	38	BLOCK	
4	4	4				PT.16 7606556	37	BLOCK	
							36		X
1	1	1				PT.15 7606556	35	COLLAR	
4	4	4				PT.14 7606556	34	SPRING	
1	1	1				NP 30407	33	NAME PLATE	
					STEEL		32	BOLTS ¼-20X3¾LG	135A
2	2	2			SEE NOTE		31	EYES-LIFTING	
☒							30	ASSEMBLY	
1						G3 7706794	29	COIL	
	☒						28	ASSEMBLY	
	1					G-2 7706794	27	COIL	
2	2	2				5# 40615	26	CLAMP	
54	54	54			#7420-14 BLACK		25	WIRE- (26 OF .010) P.I. BRAID COVERED	
40	40	40			#7420-14 BLACK		24	WIRE- (26 OF .010) P.I. BRAID COVERED	
4	4	4				PT. 2 7606556	23	INSULATOR	
2	2	2				PT. 13 7606556	22	PIN	
2	2	2			MICARTA TUBING #2A		21	BUSHING-½" OF 13/32 I.D. X ½ O.D.	61A
12	12	12			STEEL		20	SCREW- HEX. HD. MCH. SCR. 1/4-20 X 2" LG.	SEE NOTE
1	1	1				PT.13 7606309	19	TERMINAL BLOCK	
						PT. 8 7606556	18	BLOCK	
						PT. 10 7606556	17	STRIP	
						PT. 14 7606309	16	COLLAR	
4	4	4			BRASS		15	SCREW- BIND. HD. MCH. SCR. #10-32 X 1 LG	2-D
8	8	8				PT. 11 7606556	14	STRIP	
8	8	8				PT. 6 7606556	13	SLEEVE	
4	4	4				PT 1 7606556	12	BLOCK, ADJUSTING	
8	8	8				PT. 4 7606556	11	BLOCK, PILLOW.	
8	8	8				PT. 5 7606556	10	BLOCK, PILLOW	
4	4	4				PT. 3 7606556	9	BRACKET	
						PT. 8 7606556	8	SPRING	
4	4	4				PT. 7 7606556	7	SPRING	
1	1	1				PT. 12 7606556	6	STUD	
		1				G-1 7706794	5	COIL ASSEMBLY	
1	1	1				PT.3 7411203	4	COIL, FIELD	
1	1	1				PT. 2 7606555	3	COVER	SEE NOTE
1	1	1				PT. 1 7606555	2	BASE	SEE NOTE
		☒					1	ASSEMBLY	

FIG. 3 MOTOR ASSEMBLY, TYPE GS (Dwg. 7606554)

11325

elastic system is represented by the viscous damping constant, b, of Fig. 1. The viscous drag of the oil film in the small radial clearance space between the plunger and cylinder of the absorber, plus the natural damping of the absorber springs is represented by the viscous damping constant, c. The sinusoidal exciting force, $P_0 \mathrm{Sin}\,\omega t$, is supplied by the vibration motor. The actual elastic system of the experimental set-up is, therefore, exactly similar to the theoretical system of Fig. 1 on which the mathematical analysis of the absorber action is based.

6. The Vibration Fatigue Equipment.-

The vibration motor is a unit of the Westinghouse vibration fatigue equipment which is designed to vibrate mechanical systems over a frequency range of 20 to 1600 cycles per second. The output of a continously variable frequency audio oscillator is amplified by a 40 watt amplifier and delivered to the drive coil of the vibration motor. The oscillator used with this apparatus is a Hewlett-Packard audio signal generator, model 205-A, and consists of a resistance-tuned oscillator in combination with an output meter, attenuator, and an impedance matching system. The frequency output is readily varied by turning a calibrated dial. By proper adjustment the accuracy of the frequency output may be maintained within 1%. The alternating current supplied to the drive coil by the 40 watt amplifier causes the coil to oscillate in the magnetic field and develope a sinusoidally varying force which is applied to the drive rod. A simplified schematic diagram of the electrical connection of the oscillator, amplifier, and vibration motor is shown in Fig. 4, which was reproduced from the manufacture's instruction manual. The field of the vibration motor is designed for 220 volts. However, only 120 volts was used in this investigation as that was the only d.c. power readily available and

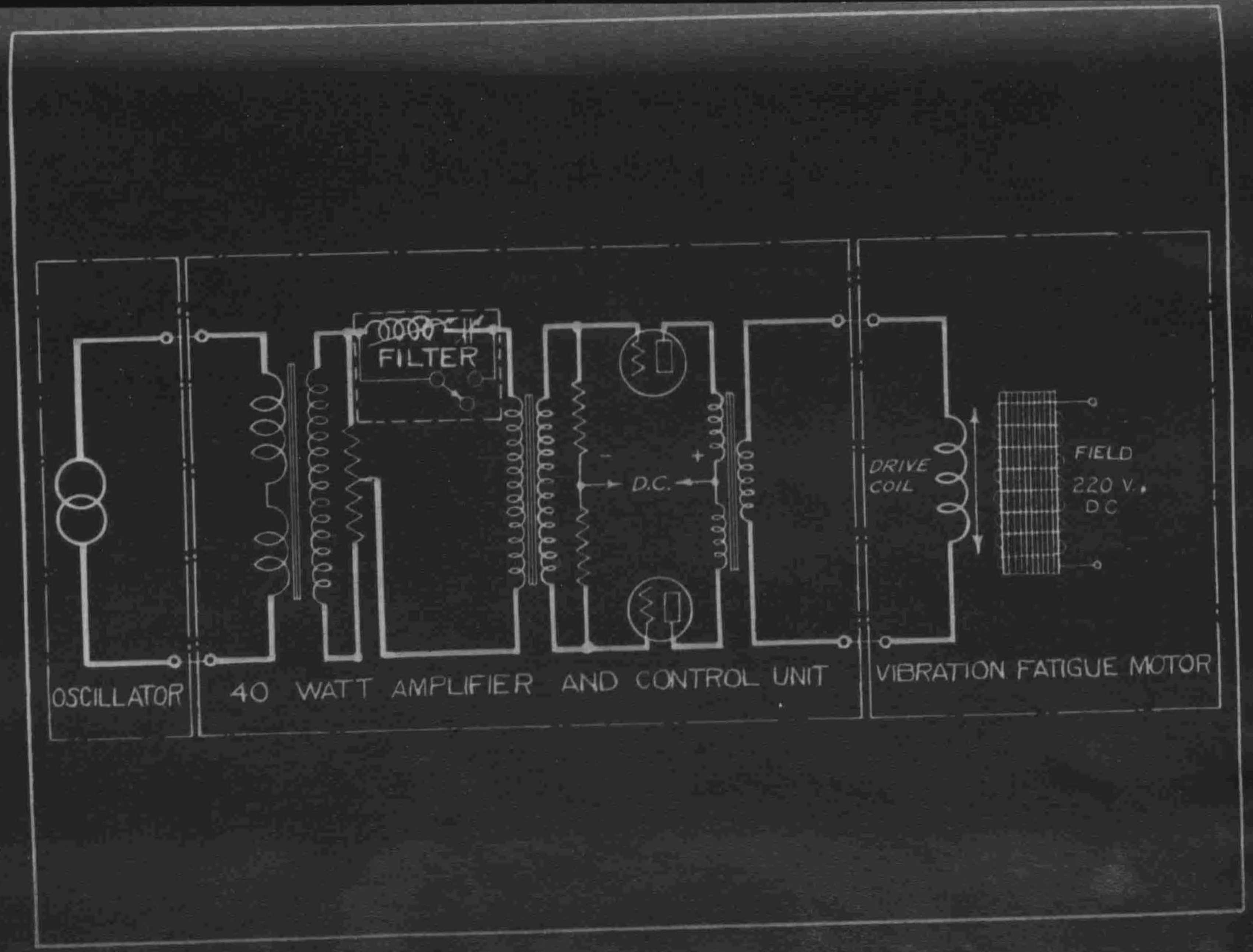

FIG. 4 SIMPLIFIED SCHEMATIC DIAGRAM, 40 WATT SYSTEM. FORCED OSCILLATION FROM EXTERNAL OSCILLATOR MANUAL AMPLITUDE CONTROL. (Dwg. 7407651)

was adequate for the purpose. The remaining power requirements of the equipment were supplied from a 115 volts, 60 cycle source.

A pick-up coil is wound on top of the drive coil of the vibration motor and is primarily intended as a feed back to the amplifier for maintaining substained self-excited oscillation, independent of the audio frequency oscillator supply, for the vibration of mechanical systems at their natural frequency. However, in this investigation it was used only to supply a signal, indicative of the amplitude and harmonic motion of the main elastic system, to oscillographs for observation and record purposes.

7. Oscillographs.-

A DuMont, type 208, cathode-ray oscillograph was used for general observation of the wave form and relative amplitude of the signal from the pick-up coil of the vibration motor. A Westinghouse, type PA, mechanical oscillograph was used for obtaining oscillograms of the die-away characteristic of the elastic system under various operating conditions. In this connection, it was found necessary to connect an audio amplifier (a Bogen, model E-30, was used) between the pick-up coil of the motor and the galvanometer element of the oscillograph in order to eliminate the undersirable damping effect of the galvanometer on the elastic system. When the signal from the pick-up coil was fed directly into the oscillograph galvanometer, the damping in the elastic system was determined to be approximately 3% of the critical damping constant, whereas, when the signal was fed through the amplifier, the damping was found to be only about 1½%. The difference between the two damping constants is indicative of the power required for driving the galvanometer element, which is in the order of 0.1 watt for full deflection.

8. Amplitude Measuring Apparatus.-

Direct measurement of the amplitude of vibration of the elastic system was obtained by means of an optical telescope and stroboscopic illumination. The telescope was mounted on the vibration motor and focused on the absorber unit near the top edge. An adjustable cross-hair with micrometer dial permitted measurement of amplitude to the nearest .0005". The stroboscopic illumination was provided by a General Radio Co. strobolux, type 648-A, triggered by a strobotac, type 631-B. By turning an illuminated calibrated dial on the strobotac, the flashing speed of the lamp in the strobolux can be accurately adjusted to any value from 10 to 100 cycles per second. When properly standarized, the accuracy of the dial reading is within 1%.

9. Arrangement of Apparatus.-

Fig. 5 shows an overall view of the apparatus. Fig. 6 gives a close up view of the vibration motor showing the mounting of the absorber unit, telescope and stroboscopic illuminator.

10. Temperature Measuring Apparatus.-

Measurement of the temperature rise of the absorber unit under various operating conditions were obtained by a copper-constantan thermocouple in conjunction with a Leeds & Northrup type K potentiometer, and a General Electric light-beam type of galvanometer. Fig. 7 shows a view of the apparatus.

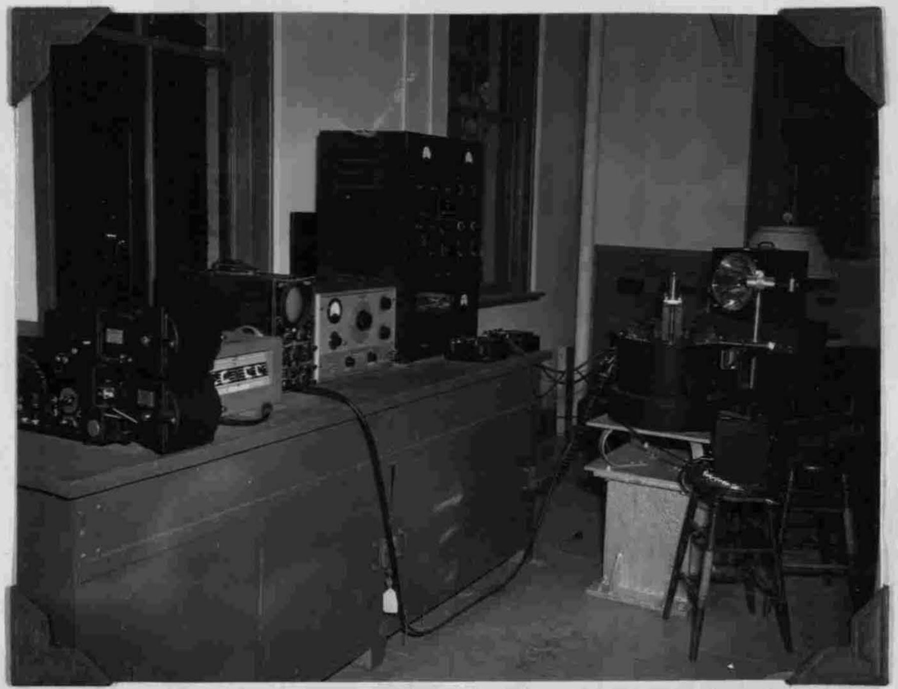

Fig. 5

Overall view of apparatus showing arrangement; from left to right, Westinghouse mechanical oscillograph, Bogen audio amplifier, DuMont cathode ray oscillograph, Hewlett-Packard oscillator, 40 watt amplifier and control unit, d.c. voltmeter and ammeter in field circuit of motor, vibration motor with absorber and telescope mounted thereon, General Radio Co. strobolux in rear with strobotac on stool in front.

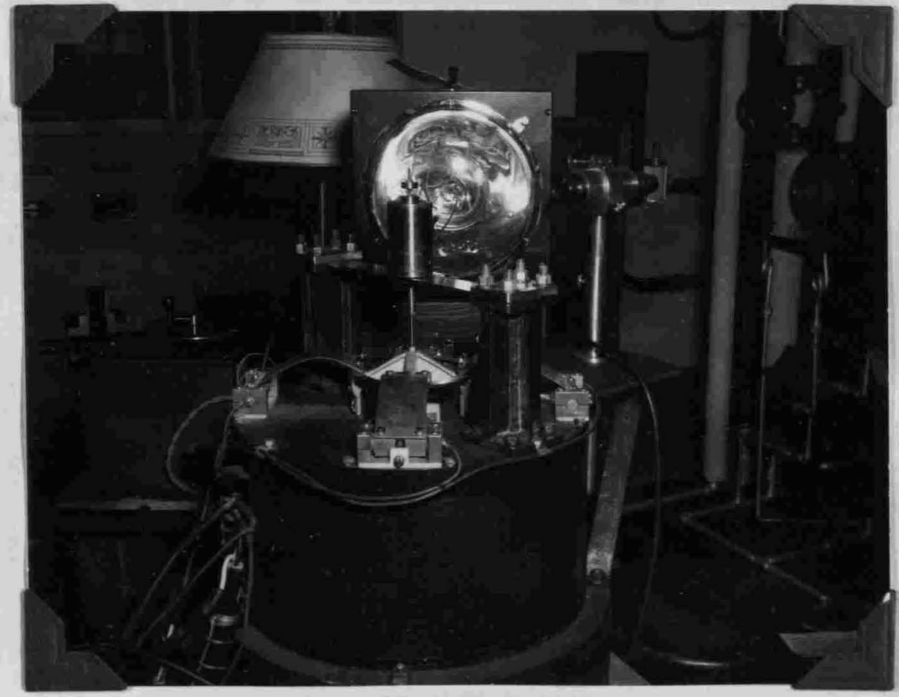

Fig. 6

Close-up of vibration motor showing mounting of absorber and telescope with strobolux on table behind motor. Note small weight secured to stem of absorber for changing from condition of constant tuning to optimum tuning.

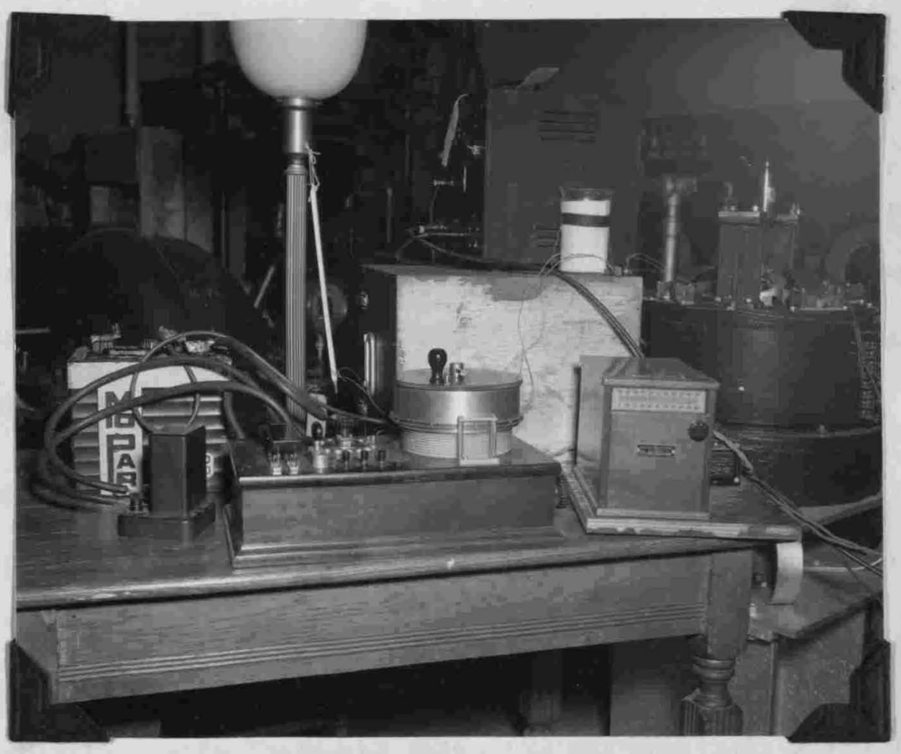

Fig. 7

Temperature measuring apparatus; from left to right, Eppley standard cell, Leeds and Northrup potentiometer, General Electric galvanometer, container for cold junction ice-water mixture on box.

CHAPTER IV

PROCEDURE AND RESULTS

1. Preliminary Considerations.-

Prior to running tests on the absorber operation, it was necessary to determine the constants of both the main elastic system and the absorber system; namely, the spring constant, mass, and natural frequency of each system. Preliminary measurements had previously been made for use in connection with the design of the absorber unit, but it was necessary to repeat all measurements using the equipment as built.

2. Main System Spring Constant.-

The spring constant of the main system, consisting of the combined effect of the fixed-ended beam with absorber unit nounted thereon and the spring suspension of the vibration motor drive coil assembly, was determined by applying static loads and measuring the resulting deflections. The static loads, consisting of 3- and 5-pound weights, were stacked on the absorber unit as shown in Fig. 8. The resulting deflections were measured to within an accuracy of one ten-thousandth of an inch (.0001") by means of an Ames, model 412, dial indicator mounted beneath the vibration motor, as shown in Fig. 9, with its indicator stem bearing against an extension of the motor drive rod. The data obtained is tabulated in Table I, and a curve of deflection vs. load is plotted on Fig. 10. The spring constant, K, is equal to the slope of the curve and was found to be 1490 lbs. per inch.

3. Absorber System Spring Constant.-

The spring constant of the absorber system was obtained by using a special jig for holding the absorber unit and dial indicator as shown in

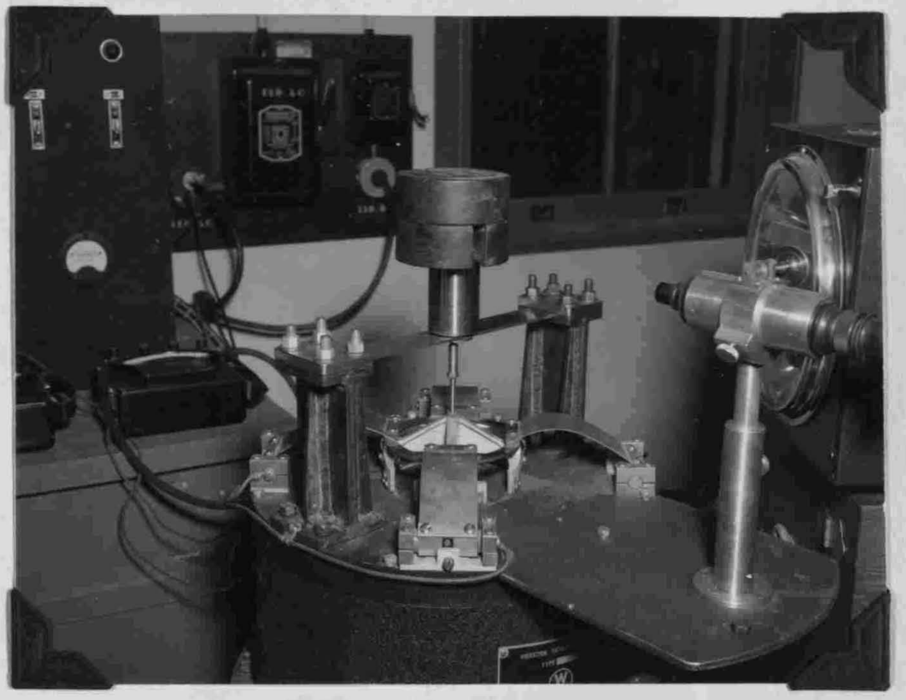

Fig. 8

Method of static loading for determination of main spring constant.

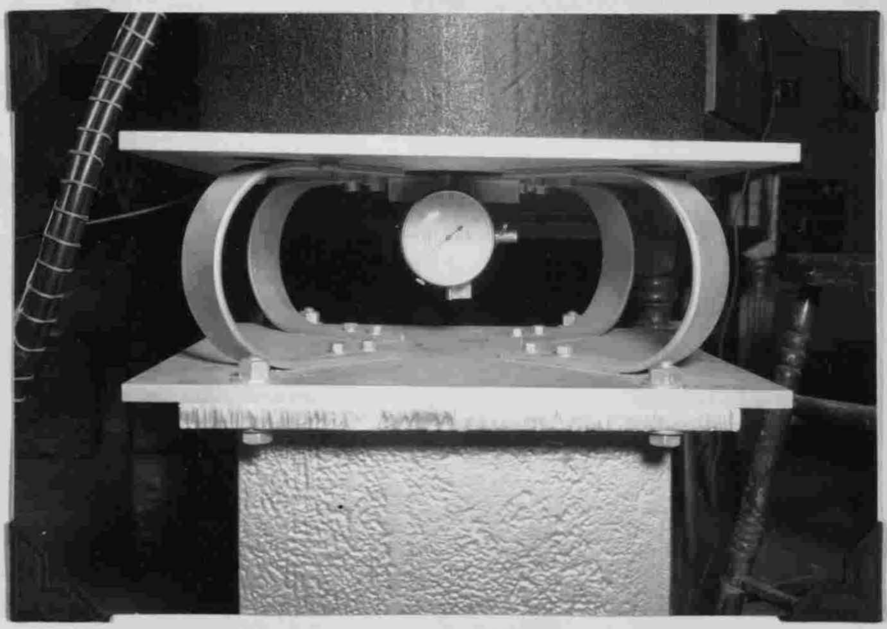

Fig. 9

Measurement of static deflection for determination of main spring constant.

TABLE I

Experimental Data for Determination of Main System Spring Constant

LOAD Lbs.	DEFLECTION Inches/10^3
0.0	0.00
3.0	2.05
5.0	3.49
8.0	5.57
10.0	6.90
13.0	8.88
15.0	10.27
18.0	12.27
20.0	13.56
23.0	15.42
25.0	16.77
28.0	18.69
30.0	19.96

Fig. 10

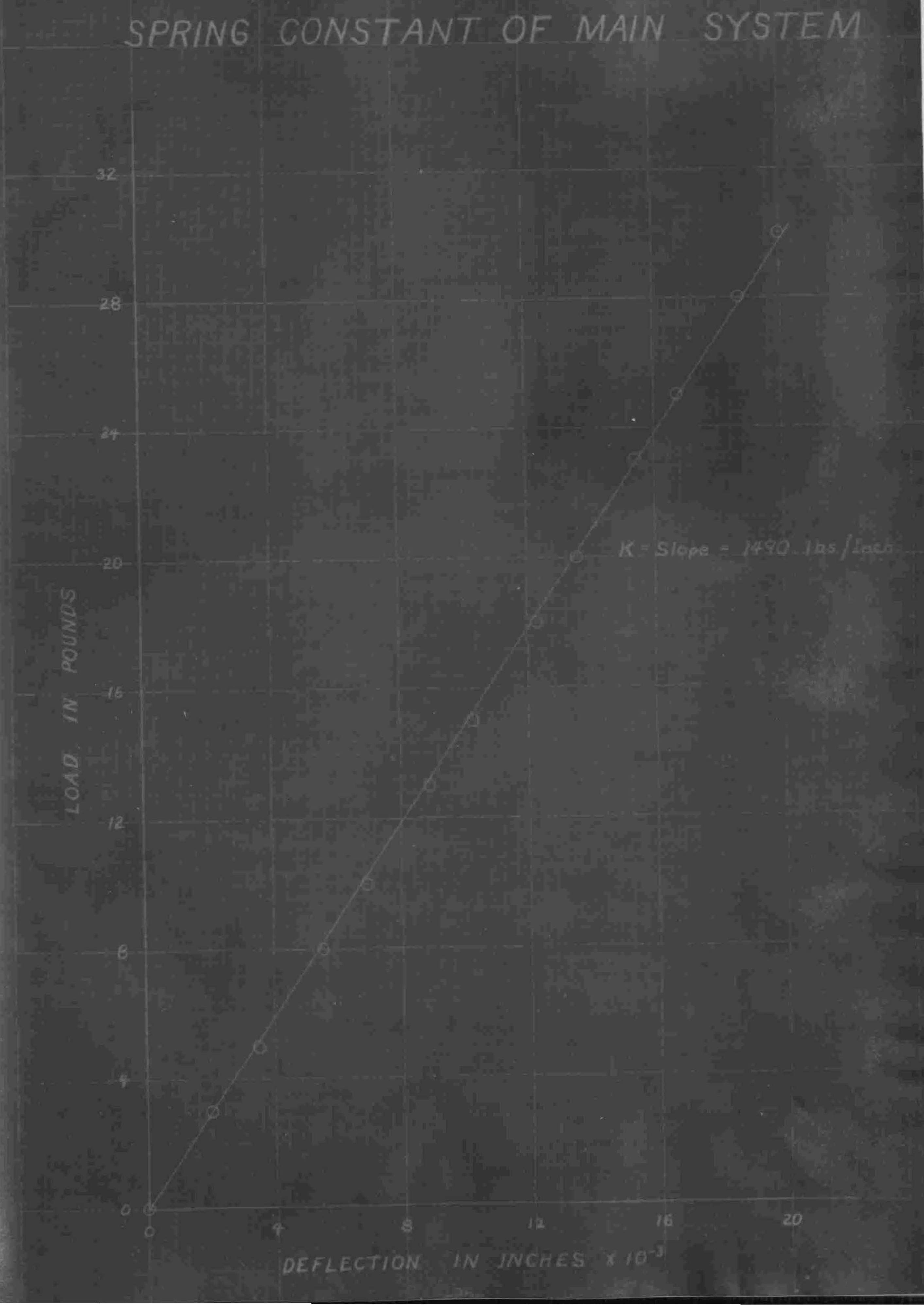
SPRING CONSTANT OF MAIN SYSTEM
K = Slope = 1490 lbs/Inch
LOAD IN POUNDS
DEFLECTION IN INCHES x 10^-3
0
4
8
12
16
20
24
28
32
0
4
8
12
16
20

Fig. 11. The static loads, consisting of 2-pound weights, were applied to the plunger rod and the resulting deflections were determined to within an accuracy of one-thousandth of an inch (.001") by an Ames, model 272, dial indicator with an extension stem bearing against the bottom end of the plunger rod. The data obtained is tabulated in Table II, and a curve of deflection vs. load is plotted on Fig. 12. The slope of the curve gives a spring constant, k, of 83.5 lbs. per inch.

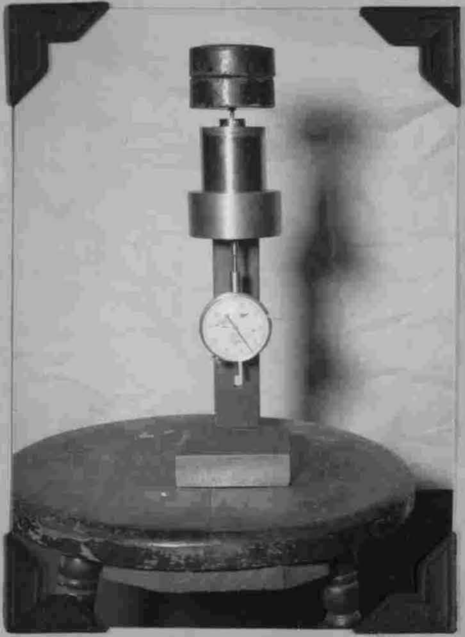

Fig. 11

4. Mass of Absorber System.-

The mass of the absorber system consists of the mass of the plunger assembly plus the inertia mass of the springs. The plunger assembly, consisting of the plunger, rod, two collars, and four nuts, was accurately weighed and found to have a mass of 0.2326 pounds. The inertia mass of the absorber springs was determined by calculating the natural frequency of one spring and using the well known formula $\omega_n = \sqrt{k_s/m_s}$, in which ω_n is the natural frequency of the spring, k_s the spring constant of one spring, and m_s the inertia mass of one spring, all in consistent units. The natural frequency of a helical steel spring is given by Wahl (5), formula (237), as $f_1 = 3510\, d/r^2n$, where f_1 is the lowest natural frequency in cycles per sec., d is the wire diameter in inches, r is the mean radius of the coil in inches, and n is the number of active turns. Using a wire diameter of 0.800", a mean coil radius (as determined by measurement) of 0.279", and 6 active turns, the natural frequency of one

TABLE II

Experimental Data for Determination of Absorber System Spring Constant

LOAD Lbs.	DEFLECTION Inches/10^3
0.0	0.0
1.0	12.1
2.0	24.1
3.0	36.0
4.0	47.9
5.0	59.9
6.0	72.0
7.0	83.9
8.0	95.8

SPRING CONSTANT OF ABSORBER SYSTEM

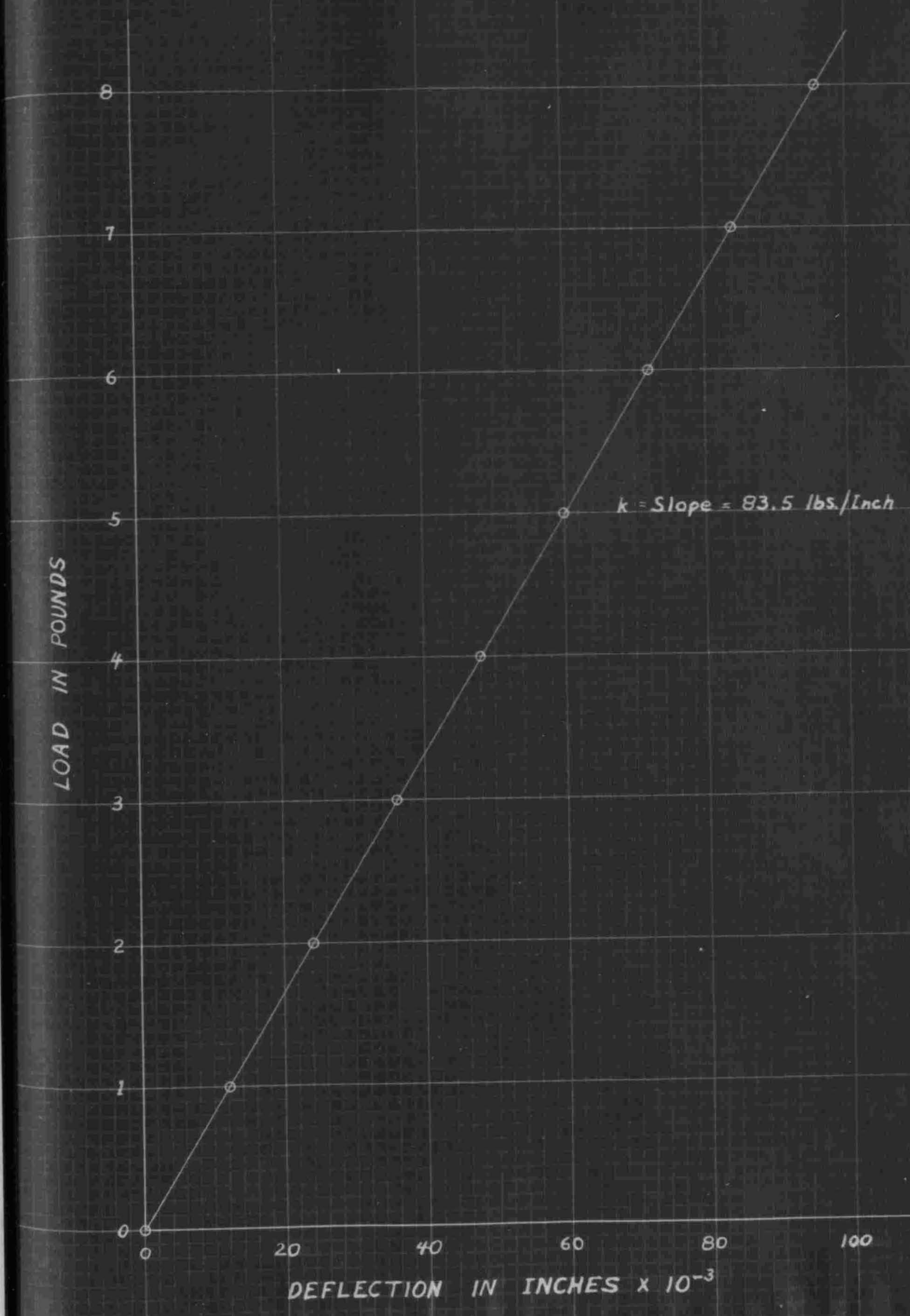

spring was computed to be 601 cycles per sec., or 3775 radians per sec. Using a spring constant of 41.75 lbs. per inch, the inertia mass of one spring, by the formula $\omega_n = \sqrt{k_s/m_s}$, is .00113 lbs; and the inertia mass of the two springs is twice this value. Therefore, the mass of the absorber system is 0.2326 + .0023 or 0.2349 pounds.

5. Natural Frequency of Absorber System.-

Knowing the mass and spring constant, the undamped natural frequency of the absorber system is readily computed by the formula $\omega_a = \sqrt{k/m}$ to be 370.4 radians per sec. or 59.0 cycles per sec.

6. Mass of Main System.-

The accurate determination of the mass of the main system presents an interesting problem. That part of the main system composed of the absorber unit (without plunger assembly), mounting fittings (consisting of extension stud, 1¼" dia. steel washer on under side of beam, and two lock nuts), and vibration motor drive coil assembly may be determined by weighing, although this procedure necessitates disassembly of the vibration motor which it was desirable to avoid if possible; in lieu thereof, average weights of the drive coil assembly were obtained from the manufacturer. The beam may be considered as a bar with fixed ends and the springs of the vibration motor (four at top and four at bottom, of spider) as cantilever beams. Root (4) shows that the inertia mass of a bar with fixed ends is equal to 0.383 times the mass of the bar, and the inertia mass of a cantilever bar is equal to 0.243 times the mass of the bar. However, the assumptions as to the end conditions of the beam and springs are undoubtly somewhat in error due to the elastic nature of the supports and other factors, and the departure of the actual conditions from the assumed conditions would be reflected in the computed inertia masses.

Another approach to the problem of determining the mass of the main system is to measure the natural frequency of the system and, knowing the spring constant, compute the mass, M, from the formula, $\Omega_n = \sqrt{K/M}$. However, this method presupposes neligible damping in the system since the damped natural frequency of a simple elastic system is given by the formula, $Q = \sqrt{K/M - (b/2M)^2}$. The damping constant, b, was determined, in a manner to be described later, to be of the order of 1½% of the critical damping. By substituting approximate values in the damped natural frequency formula, it may be shown that the damping term, $(b/2M)^2$, is less than a tenth of one percent of the main term, K/M. Therefore, to the limit of experimental accuracy, the mass of the main system may safely be computed from the formula, $\Omega_n = \sqrt{K/M}$. By using this method it was found necessary to add only 0.095 lbs. (41.2 grams) to the main mass system in order to bring the system into the condition of constant tuning, $\omega_a = \Omega_n = 59.0$ cycles per sec. For this condition, the mass of the main system is readily computed to be 4.193 pounds.

7. Summary of System Constants.-

For ready reference, the basic constants of the system under investigation, for the case of constant tuning, $f = 1$, are tabulated below:

$K = 1490$ lbs./inch

$M = 4.193$ lbs.

$\Omega_n = \omega_a = 370.4$ rad./sec. $= 59.0$ c.p.s.

$k = 83.5$ lbs./inch

$m = 0.2349$ lbs.

$\mu = m/M = .0560$

Optimum tuning will, theoretically, occure when equation (23) is satisfied; namely, when $f = 1/(1 + \mu)$. By the method of successive approximations, using the formulas, $\mu = m/M$, $f = 1/(1 + \mu)$, $\omega_a = f\,\Omega_n$, and $m = k/\omega_a^2$, the following constants are readily computed for the case of optimum tuning:

$m = 0.2657$ lbs.
$\mu = m/M = .0633$
$f = 1/(1 - \quad) = .9404$
$\omega_a = f\,\Omega_n = 348.3$ rad./sec. = 55.5 c.p.s.

Therefore, the system may be changed from the condition of constant tuning to that of optimum tuning by merely adding .0308 lbs. (14.0 grams) to the plunger rod of the absorber.

8. Amplitude Response Tests.-

Knowing the constants of the system, we are now in a position to devise tests for verification of the theory developed in Chapter II. Briefly, the tests which were conducted consisted of measuring the amplitude of vibration of the main mass over a frequency range from 26 to 96 cycles per sec. ($g = .441$ to 1.627) for each of four different damping conditions for both the case of constant tuning and that of optimum tuning. For each chosen frequency setting and operating condition, the peak to peak amplitude of vibration of the main mass was obtained by adjusting the frequency of the flashing of the stroboscopic lamp until the mass appeared to be moving up and down at a very slow rate. Then, by observing through the telescope the motion of a scribe mark (placed near the top of the absorber unit), setting the adjustable cross-hair to coinside with first the upper and then the lower limit of travel of the scribe mark, reading the micrometer adjustment dial for each position, the peak-to-peak amplitude was determined to within an accuracy of .0005". It was found that the cross-hair adjustment dial moved through 222 scale divisions for each 0.100" travel of the cross-hair; therefore, each division on the dial represents .00045".

The absorber damping constant, c, was varied by using oils of different viscosity in the clearance space between the absorber plunger and cylinder The viscosity data, as furnished by the U. S. Naval Engineering Experiment Station, for the three oils used is tabulated and plotted on Fig. 13. The infinite damping condition was obtained by locking the plunger in place.

For comparison with the theory of Chapter II, it is desirable to plot the experimental results in the form of dimensionless curves with the driving frequency ratio, $g = \omega/\Omega_n$, as the independent variable along the abscissa, and the amplitude ratio of the main system, x_1/x_0, as the dependent variable along the ordinate axis. The driving frequency ratio is readily obtained by dividing the frequency setting for each observation by the natural frequency of the main mass system, $\Omega_n = 59.0$ cycles per second. In order to obtain the amplitude ratio, it is necessary to determine the statical deflection of the main system, x_0. One method would be to plot an (ω, x_1) curve in the low frequency region for the case of c equal to infinity (plunger locked). By inspection of equation (11), which is applicable to this condition, it is apparent that as g approaches zero, x_1/x_0 approaches unity. Therefore, the ordinate of the point where the curve levels out at zero frequency would represent x_0. However, since the lower limit of the oscillator frequency is 20 cycles per sec. and it is difficult to extrapolate the (ω, x_1)

Fig. 13

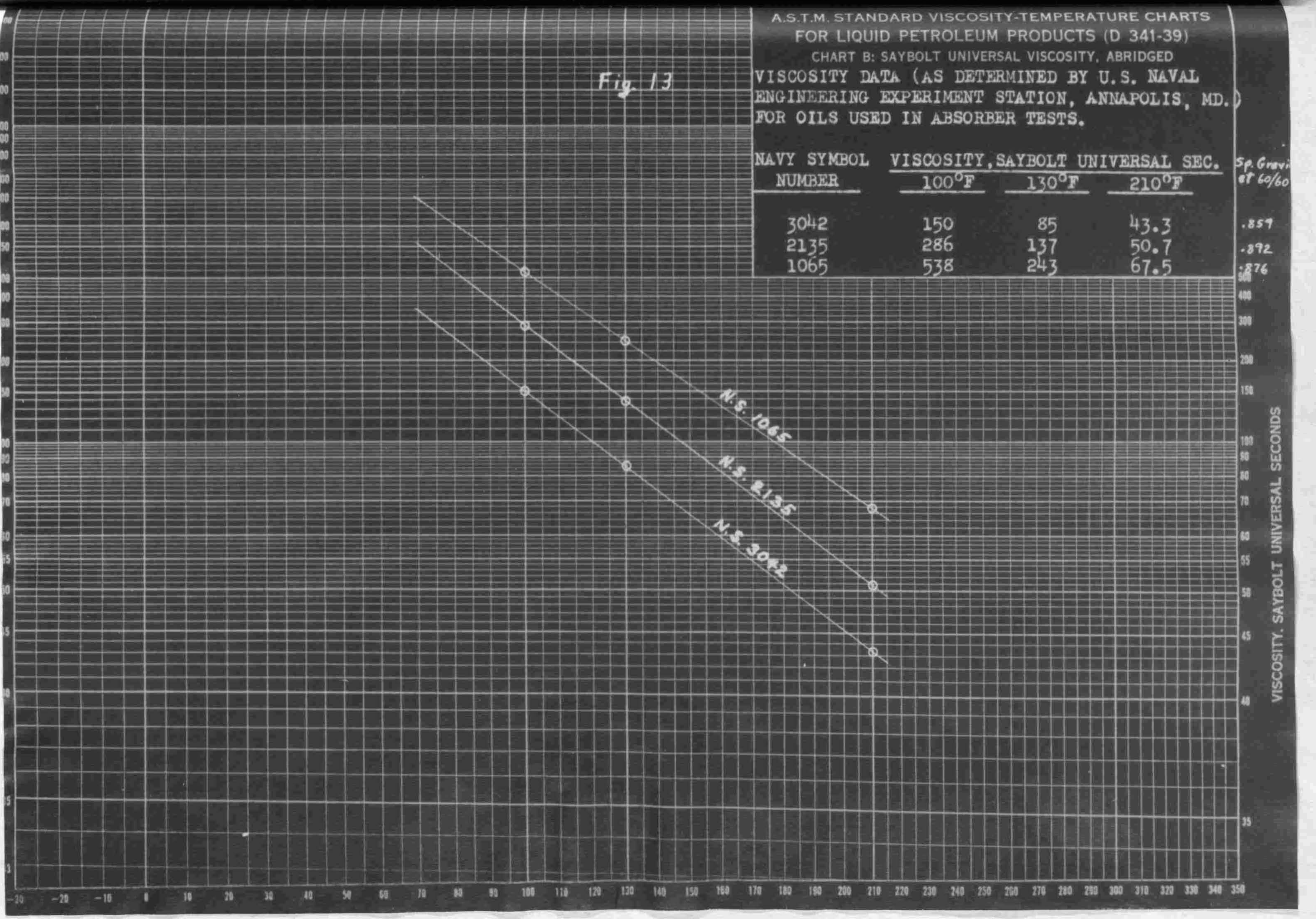

A.S.T.M. STANDARD VISCOSITY-TEMPERATURE CHARTS FOR LIQUID PETROLEUM PRODUCTS (D 341-39)

CHART B: SAYBOLT UNIVERSAL VISCOSITY, ABRIDGED

VISCOSITY DATA (AS DETERMINED BY U.S. NAVAL ENGINEERING EXPERIMENT STATION, ANNAPOLIS, MD.) FOR OILS USED IN ABSORBER TESTS.

NAVY SYMBOL NUMBER	VISCOSITY, SAYBOLT UNIVERSAL SEC.			Sp. Gravi at 60/60
	100°F	130°F	210°F	
3042	150	85	43.3	.859
2135	286	137	50.7	.892
1065	538	243	67.5	.876

curve to zero frequency with sufficient precision, a more accurate method was devised. Again inspecting equation (11), it will be noted that as g approaches infinity, x_1/x_0 approaches zero. Therefore, there must be a point in the upper frequency region at which the $(g, x_1/x_0)$ curve intersects the line $x_1/x_0 = 1$, and the value of g at which this occures is readily computed. This method of determining x_0 is illustrated on Fig. 14 and the data for plotting the (ω, x_1) curve is tabulated in Table III. The statical deflection, x_0, was thus found to be 7.3 units, where one unit represents the distance traversed by the cross-hair of the telescope when the micrometer dial is turned through one division.

All tests were run with the same output level setting on the oscillator, so that the input to the motor drive coil was constant. Also, the d.c. voltage across the motor field was maintained constant within 1%. Therefore, the statical deflection, x_0, as determined above may be considered a constant, and the amplitude ratio, x_1/x_0, is readily computed for each observation.

Prior to the start of each test, adequate warm-up time was allowed for temperature stabilization of the equipment and oil film in the radial clearance space between the absorber plunger and cylinder.

The experimental data for a series of curves for the case of constant tuning is tabulated in Table IV and the curves are plotted on Fig. 15. Similarily, for the case of optimum tuning, the data is tabulated in Table VI and the curves are plotted on Fig. 16.

9. Theoretical Curves.-

For comparison purposes, theoretical curves were calculated and plotted on the same graphs as the experimental curves, Figs. 15 and 16. Equation (11) was used for computing the curve of infinite damping for

TABLE III

Experimental Data for Determination of Static Displacement of Main System

$f = 1$, $c = \infty$

ω cycles/sec.	x_1
64.0	27.0
66.0	21.0
68.0	17.5
70.0	14.0
73.0	11.0
76.0	9.5
79.0	8.0
82.0	7.0
85.0	6.0
88.0	5.0
92.0	4.5
96.0	4.0

Fig 17

DETERMINATION OF STATIC DISPLACEMENT OF MAIN SYSTEM

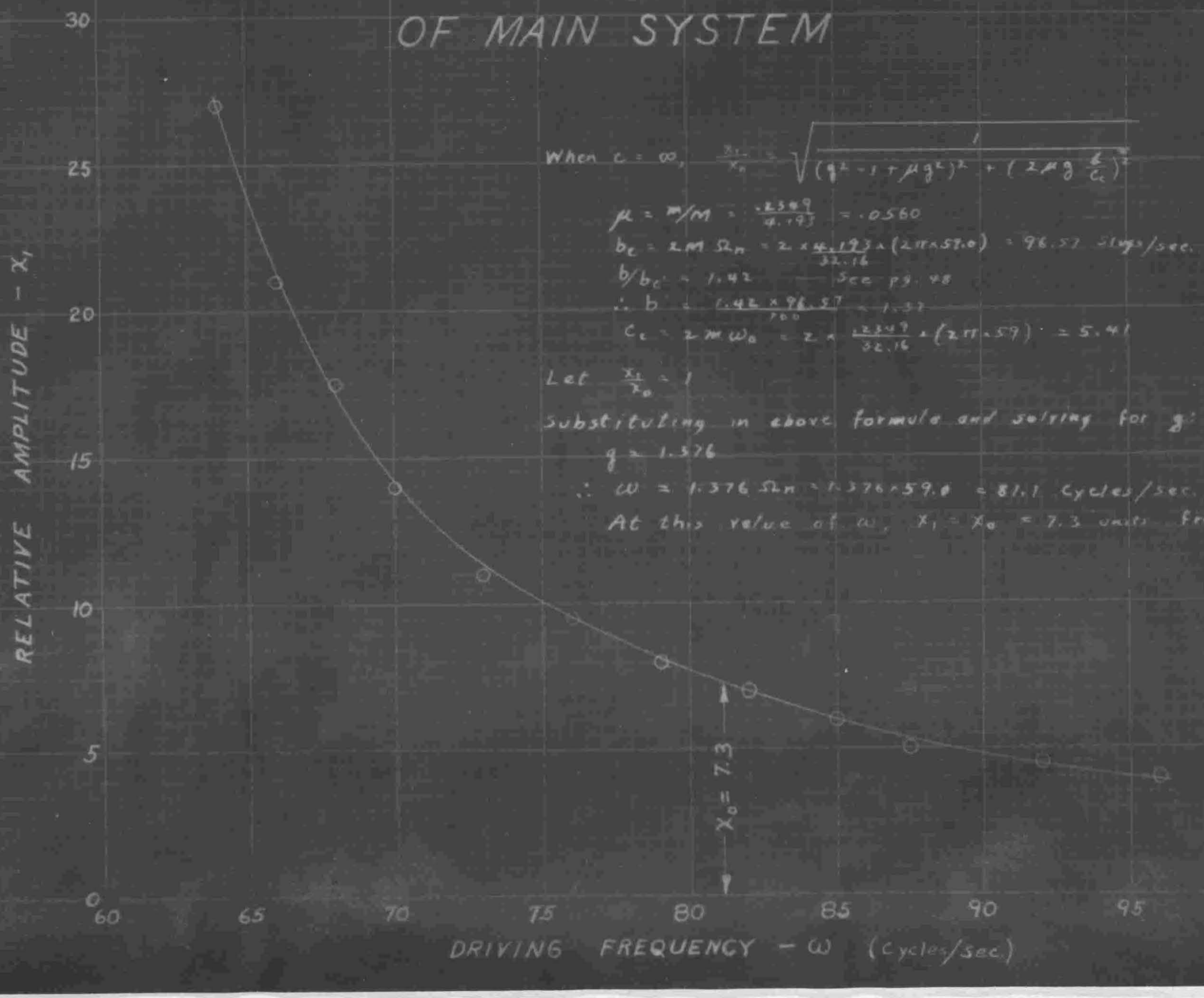

When $c = \infty$, $\frac{x_1}{x_0} = \sqrt{\frac{1}{(g^2 - 1 + \mu g^2)^2 + (2 \mu g \frac{b}{c_c})^2}}$

$\mu = m/M = \frac{.2349}{4.193} = .0560$

$b_c = 2 M \Omega_n = 2 \times \frac{4.193}{32.16} \times (2\pi \times 59.0) = 96.57$ Slugs/sec.

$b/b_c = 1.42$ — See pg. 48

$\therefore b = \frac{1.42 \times 96.57}{100} = 1.37$

$c_c = 2 m \omega_0 = 2 \times \frac{.2349}{32.16} \times (2\pi \times 59) = 5.41$

Let $\frac{x_1}{x_0} = 1$

Substituting in above formula and solving for g:

$g = 1.376$

$\therefore \omega = 1.376 \Omega_n = 1.376 \times 59.0 = 81.1$ Cycles/sec. $= 510$ Rad/sec.

At this value of ω, $X_1 = X_0 = 7.3$ units from curve

TABLE IV

Experimental Data for Case of Constant Tuning

ω cycles/sec.	g	x_1/x_0 Plunger locked	Oil #3042	Oil #2135	Oil #1065
26.0	0.441	1.17	1.23	1.17	1.17
29.0	0.492	1.23	1.37	1.23	1.30
32.0	0.542	1.37	1.51	1.33	1.37
35.0	0.593	1.51	1.64	1.37	1.51
38.0	0.644	1.65	1.78	1.72	1.72
40.0	0.678	1.78			
41.0	0.695		2.06	2.06	1.92
42.0	0.712	1.92			
44.0	0.746	2.19	2.46	2.47	2.26
46.0	0.780	2.54	3.02	3.08	2.61
48.0	0.814	3.08	3.70	3.84	3.15
49.0	0.830		4.52		
50.0	0.848	4.04	5.21	5.07	3.98
51.0	0.865	4.59	5.75		
52.0	0.882	5.41	6.30	6.64	5.41
53.0	0.899	6.85	6.58	7.40	6.44
54.0	0.916	8.15	6.44	7.68	7.81
55.0	0.932	14.80	6.03	7.40	9.32
56.0	0.949	22.20	5.48	6.85	10.29
57.0	0.966	33.83	5.20	6.30	10.02
57.4	0.973	35.89			
57.7	0.979	34.65			
58.0	0.983	21.92	4.93	5.69	9.26
59.0	1.000	12.21	4.66	5.21	7.96
60.0	1.017	8.63	4.38	4.80	6.58
61.0	1.034	6.71			
62.0	1.051	5.34	4.11	4.04	4.93
64.0	1.068	3.90	3.84	3.42	3.77
66.0	1.119	3.02	3.42	2.88	3.02
68.0	1.153	2.40	2.88	2.47	2.47
70.0	1.186	1.92	2.33	2.06	2.06
72.0	1.220		2.05	1.78	1.78
73.0	1.237	1.51			
75.0	1.271		1.64	1.51	1.51
76.0	1.288	1.30			
78.0	1.322		1.37	1.23	1.23
79.0	1.339	1.10			
81.0	1.373		1.23	0.96	0.96
82.0	1.390	0.96			
84.0	1.424		1.10	0.80	0.82
85.0	1.441	0.82			
87.0	1.475		0.96	0.73	0.75
88.0	1.492	0.69			
90.0	1.525		0.89	0.69	0.69
92.0	1.560	0.62			
93.0	1.576		0.82	0.62	0.62
96.0	1.627	0.55	0.75	0.55	0.55
Ave. ambient temp. - °F			75.0	77.7	78.0
Ave. d.c. field volts		116.0	116.1	116.8	115.7
Ave. d.c. field amps.		0.79	0.80	0.82	0.80

TABLE V

Points for Plotting Theoretical Curve for Case of Constant Tuning and Infinite Damping ($f = 1$, $c = \infty$) as Calculated by Formula (11):

$$\frac{x_1}{x_0} = \sqrt{\frac{1}{(g^2 - 1 + \mu g^2)^2 + \left(2\mu g \frac{b}{C_c}\right)^2}}$$

$\mu = .05602$

$b = 1.382$ slugs/sec.

$C_c = 5.409$ slugs/sec.

g	x_1/x_0
0.450	1.31
0.500	1.36
0.550	1.47
0.600	1.61
0.650	1.80
0.700	2.07
0.750	2.46
0.800	3.08
0.850	4.20
0.900	6.80
0.925	9.97
0.950	18.57
0.960	25.98
0.970	34.77
0.9731	35.89
0.975	35.40
0.980	31.73
0.990	22.18
1.000	16.01
1.050	5.99
1.100	3.57
1.150	2.51
1.200	1.92
1.250	1.54
1.300	1.27
1.350	1.08
1.400	0.93
1.450	0.82
1.500	0.73
1.550	0.65
1.600	0.59

Fig 15

CURVES FOR CONSTANT TUNING

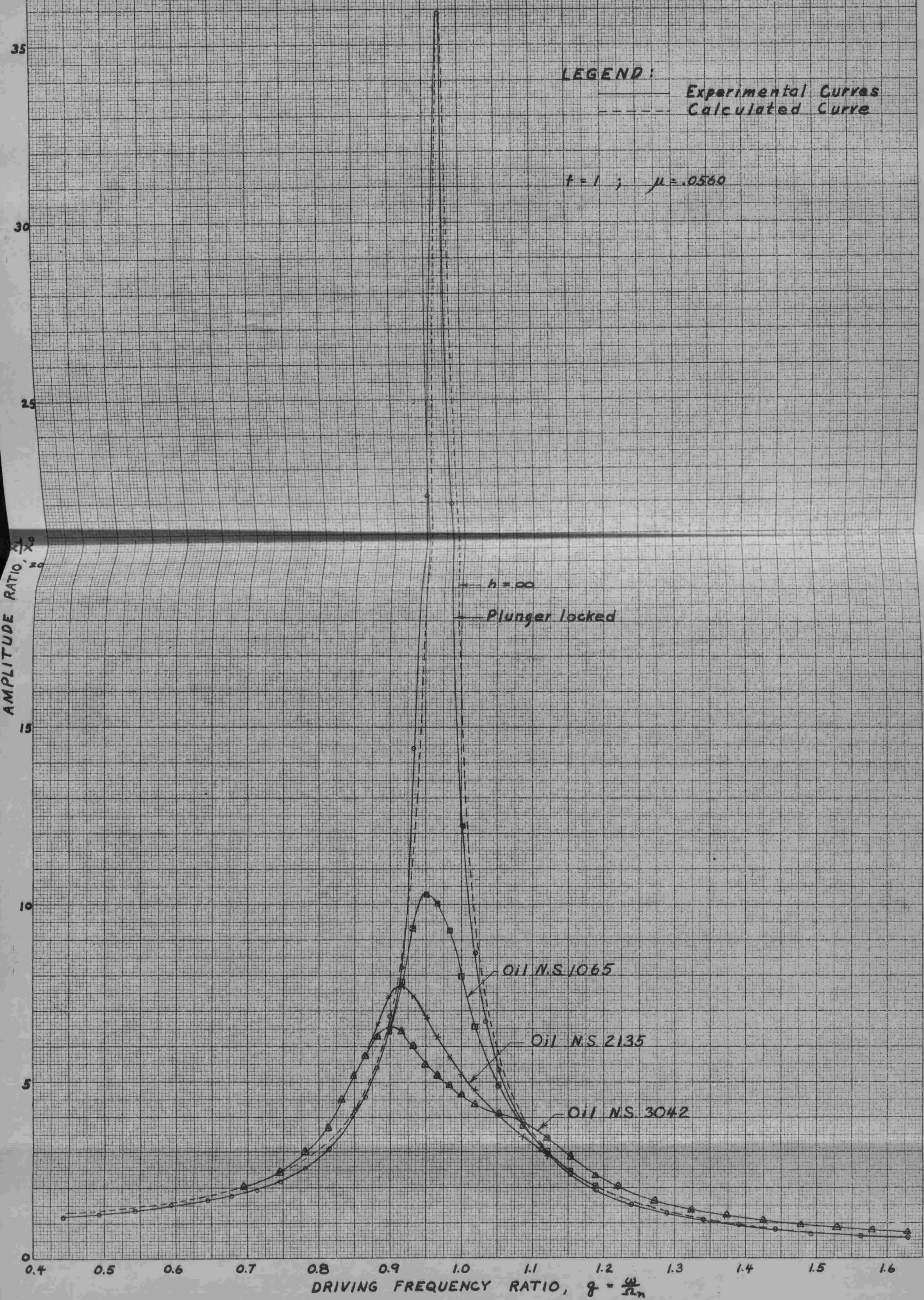

TABLE VI

Experimental Data for Case of Optimum Tuning

ω	g	x_1/x_0			
cycles/sec.		Plunger locked	Oil #3042	Oil #2135	Oil #1065
26.0	0.441	1.10	1.17	1.17	1.17
29.0	0.492	1.23	1.30	1.23	1.23
32.0	0.542	1.37	1.44	1.37	1.30
35.0	0.593	1.51	1.58	1.51	1.51
38.0	0.644	1.71	1.71	1.78	1.64
40.0	0.678	1.85			
41.0	0.695		2.06	2.05	1.92
42.0	0.712	2.06			
44.0	0.746	2.33	2.56	2.53	2.26
46.0	0.780	2.67	3.15	3.15	2.60
48.0	0.814	3.15	3.97	3.97	3.08
49.0	0.830		4.66		
50.0	0.848	3.97	5.00	4.86	3.77
51.0	0.865	4.59	5.00		
52.0	0.882	5.48	4.52	5.68	4.93
53.0	0.899	6.65	4.11		5.82
54.0	0.916	9.18	3.77	5.75	6.78
55.0	0.932	15.48	3.63		7.81
56.0	0.949	24.32	3.42	5.68	8.77
57.0	0.966	34.25	3.49		9.04
57.2	0.970	35.75			
58.0	0.983	17.81	3.70	5.48	8.90
59.0	1.000	11.24	3.91		7.81
60.0	1.017	8.44	4.11	4.93	6.85
61.0	1.034	6.58	4.46		6.03
62.0	1.051	5.28	4.87	4.38	5.14
63.0	1.068		5.00		
64.0	1.085	3.77	5.00	3.77	4.04
65.0	1.102		4.79		
66.0	1.119	2.95	4.52	3.15	3.29
67.0	1.136		3.97		
68.0	1.153	2.40	3.56	2.53	2.67
69.0	1.170		3.08		
70.0	1.186	1.92	2.74	2.26	2.19
72.0	1.220		2.26	1.99	1.92
73.0	1.237	1.65			
74.0	1.254		1.92	1.71	
75.0	1.271				1.51
76.0	1.288	1.37	1.58	1.51	
78.0	1.322		1.37	1.30	1.23
79.0	1.339	1.10			
81.0	1.373		1.17	1.03	1.03
82.0	1.390	0.96			
84.0	1.424		1.03	0.89	0.89
85.0	1.441	0.82			
87.0	1.475		0.96	0.82	0.75
88.0	1.492	0.69			
90.0	1.525		0.82	0.75	0.69
92.0	1.560	0.62			
93.0	1.576		0.69	0.69	0.62
96.0	1.627	0.55	0.62	0.62	0.55
Ave. ambient temp. - °F			80.0	80.0	78.7
Ave. d.c. field volts		115.4	116.3	116.8	116.1
Ave. d.c. field amps.		0.80	0.82	0.82	0.81

TABLE VII

Points for Plotting Theoretical Curve for Case of Optimum Tuning and Infinite Damping ($f = .9404$, $c = \infty$) as Calculated by Formula (11):

$$\frac{x_1}{x_0} = \sqrt{\frac{1}{(q^2 - 1 + \mu q^2)^2 + (2 \mu q \frac{b}{C_c})^2}}$$

$\mu = .0633$, $b = 1.393$ slugs/sec., $C_c = 6.120$ slugs/sec.

g	x_1/x_0
0.450	1.27
0.500	1.36
0.550	1.47
0.600	1.62
0.650	1.81
0.700	2.09
0.750	2.48
0.800	3.12
0.850	4.29
0.900	7.09
0.925	10.63
0.950	20.51
0.960	29.27
0.9698	35.75
0.975	33.17
0.980	28.27
0.990	19.63
1.000	14.36
1.050	5.71
1.100	3.47
1.150	2.46
1.200	1.88
1.250	1.51
1.300	1.25
1.350	1.07
1.400	0.92
1.450	0.81
1.500	0.72
1.550	0.64
1.600	0.58

TABLE VIII

Points for Plotting Theoretical Curves for Case of Optimum Tuning as Calculated by Formula (9):

$$\frac{x_1}{x_0} = \sqrt{\frac{(2hg^{2} + (g^2-f^2)^2}{(2hg)^2\left[g^2-1+\mu g^2+\mu\frac{b}{c}(g^2-f^2)\right]^2+\left[\mu f^2 g^2-(g^2-1)(g^2-f^2)+4\mu h g^2\frac{b}{C_c}\right]^2}}$$

$f = 0.9404$, $\mu = .0633$, $b = 1.393$ slugs/sec., $C_c = 6.120$ slugs/sec.

g	x_1/x_0 h = 0.1	 h = 0.2	 h = 0.3
0.750	2.83	2.68	2.61
0.800	3.92	3.45	3.28
0.825	4.80	3.96	3.76
0.850	5.41	4.54	4.37
0.875	5.22	5.12	5.15
0.900	4.34	5.58	6.18
0.925	3.62	5.83	7.24
0.950	3.29	5.89	7.97
0.975	3.31	5.83	8.03
1.000	3.62	5.68	7.26
1.025	4.16	5.40	6.18
1.050	4.83	5.00	5.16
1.075	5.34	4.53	4.29
1.100	5.29	3.98	3.65
1.125	4.71	3.46	3.14
1.150	4.01	3.06	2.74
1.200	2.83	2.36	2.14
1.250	2.19	1.93	1.76

0.6 – 1.672
0.7 – 1.755
.8 –
.9 – 2.39
1.0 – 3.68
1.1 – 4.40
1.2 –
1.3 – 2.12

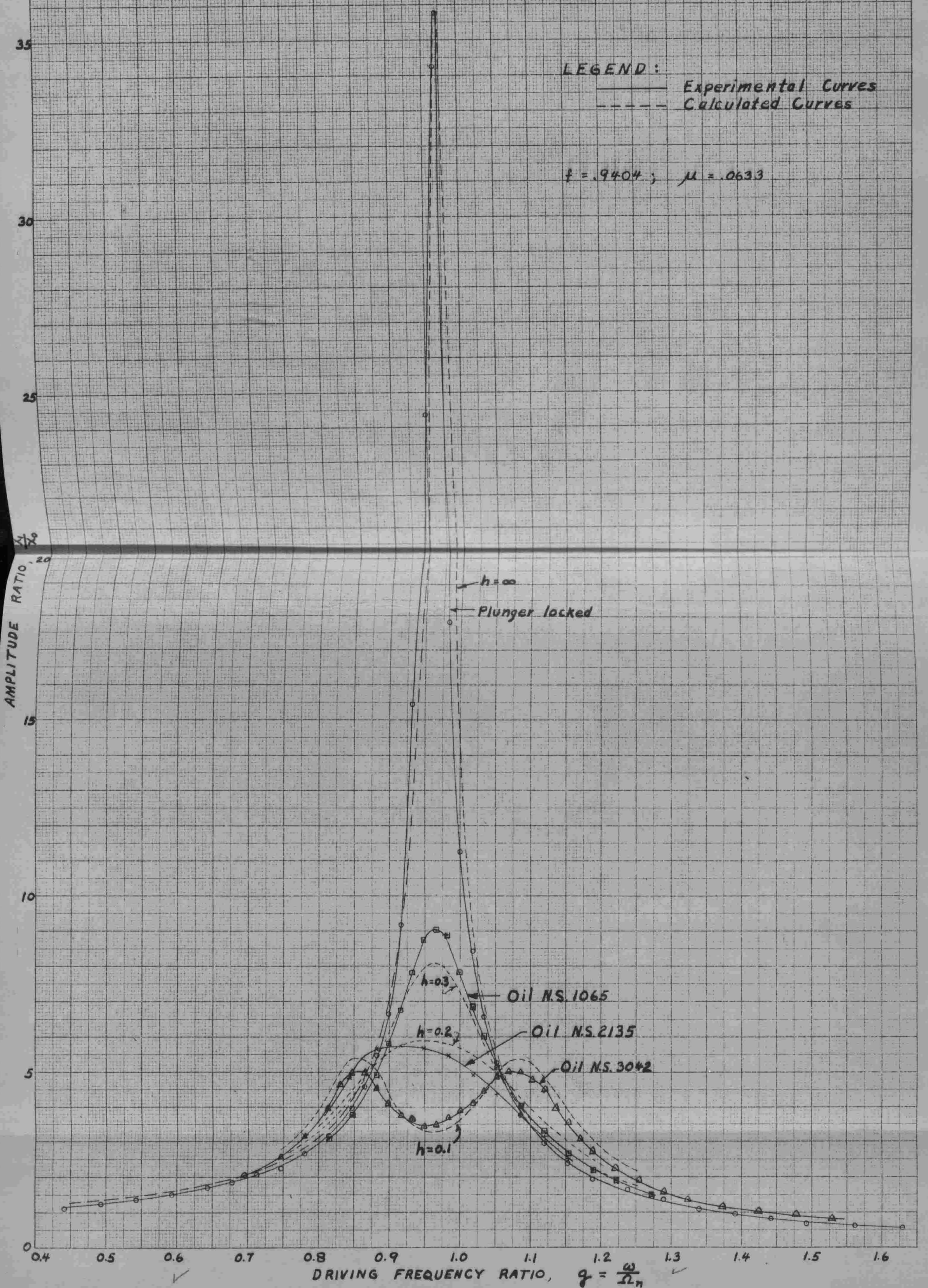

Fig. 16

CURVES FOR OPTIMUM TUNING

both tuning conditions. For each case the main system damping constant, b, was computed from equation (11) by substituting the peak value of x_1/x_0 from the experimental curve and solving for b, thus making the peak of the computed and experimental curves coincide. The calculated points for plotting the curves are tabulated in Tables V and VII.

Equation (9) was used for computing theoretical curves to show the effect of the damping ratio, $h = c/c_c$. For the case of optimum tuning, curves were computed for $h = 0.1$, 0.2, and 0.3, and the points so calculated are tabulated in Table VIII.

10. Absorber Temperature Rise.-

The absorber damping constant, c, varies directly with the viscosity of the oil film in the clearance space between the plunger and cylinder, which in turn is a function of the temperature. An indication of the temperature of the oil film may be obtained by measuring the outside surface temperature of the absorber cylinder. This was accomplished by soldering a calibrated copper-constantan thermocouple to the surface of the absorber cylinder, using an ice-water mixture for the cold junction, and measuring the millivolts generated in the junction by means of a galvanometer and associated apparatus described in section 10 of Chapter III and pictured in Fig. 7. A test was run on each of the three oils used in the amplitude tests, taking readings every five minutes until the temperature was stabilized. All tests were run for the constant tuning condition and with the driving frequency set at the point which gave the greatest relative motion between the plunger and cylinder. Corresponding measurements were also made on a second thermocouple suspended in the free air several feet from the vibration apparatus, and a mercury thermometer was used as a check on the ambient temperature.

The millivolt measurements were converted to temperature by using the calibrated data supplied by the manufacturer of the thermocouple wire, the Leeds & Northrup Co. The results of the tests are tabulated in Table IX and plotted on Fig. 17.

11. Main System Damping Constant.-

As an independent check on the damping constant of the main system, an oscillogram was taken of the die-away characteristic for the condition $f = 1$, $c = \infty$, and the damping constant was computed by the logarithmic decrement method. The oscillogram and computations are shown on Fig. 18. The reader is refered to Den Hartog (3) or other standard text on vibrations for an explanation of the theory of the logarithmic decrement method.

12. Oscillograms.-

As a matter of general interest, oscillograms were taken of the die-away characteristics of the system with the absorber in operation for the case of optimum tuning for each of the three oils used in the amplitude tests. In each case the system was operated at the natural frequency of the main mass system, $\Omega_n = 59.0$ c.p.s., prior to opening the drive coil circuit. Also, the amplifier gain setting of the signal to the oscillograph was held constant so that the oscillograms would be comparable on an amplitude basis. The results obtained are shown in Figs. 19, 20, and 21.

TABLE IX

Experimental Data for Absorber Temperature Rise Curves

Time in Minutes	Oil #3042 Temperature °F		Oil #2135 Temperature °F		Oil #1065 Temperature °F	
	Ambient	Absorber	Ambient	Absorber	Ambient	Absorber
0	79.2	78.3	78.3	78.3	77.5	77.9
5	79.2	79.0	78.3	78.8	77.5	78.9
10	79.5	79.5	78.3	79.2	77.5	79.5
15	79.5	79.7	78.3	79.5	77.7	79.7
20	79.2	79.9	78.3	79.7	77.7	80.1
25	79.5	80.1	78.3	79.9	77.5	80.6
30	79.5	80.3	77.9	79.9	77.5	81.0
35	79.5	80.6	78.1	80.1	77.3	81.2
40	79.5	80.8	77.9	80.1	77.3	81.5
45	79.5	81.0	77.9	80.4	77.5	81.7
50	79.2	81.2	78.1	80.6	77.5	81.9
55	79.2	81.2	78.1	80.8	77.5	81.9
60	79.2	81.4	78.3	80.8	77.5	82.1
65	79.5	81.4	78.6	81.0	77.5	82.1
70	79.2	81.6	78.3	81.2	77.5	82.4
75	79.5	81.6	78.3	81.2	77.5	82.4
80	79.2	81.6	77.9	81.2	77.5	82.4

Fig. 17

ABSORBER TEMPERATURE RISE CURVES

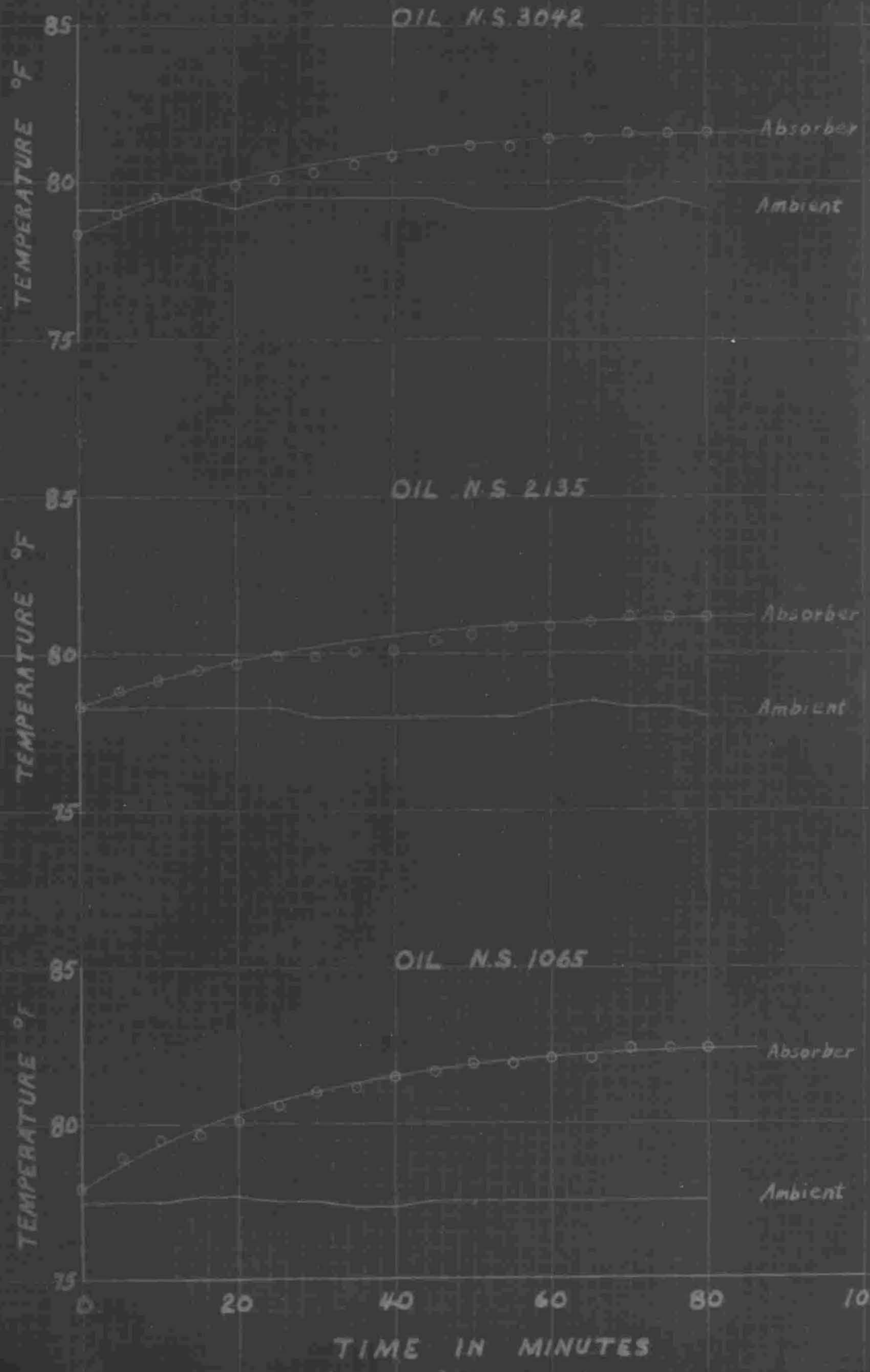
OIL N.S.3042

OIL N.S. 2135

OIL N.S. 1065

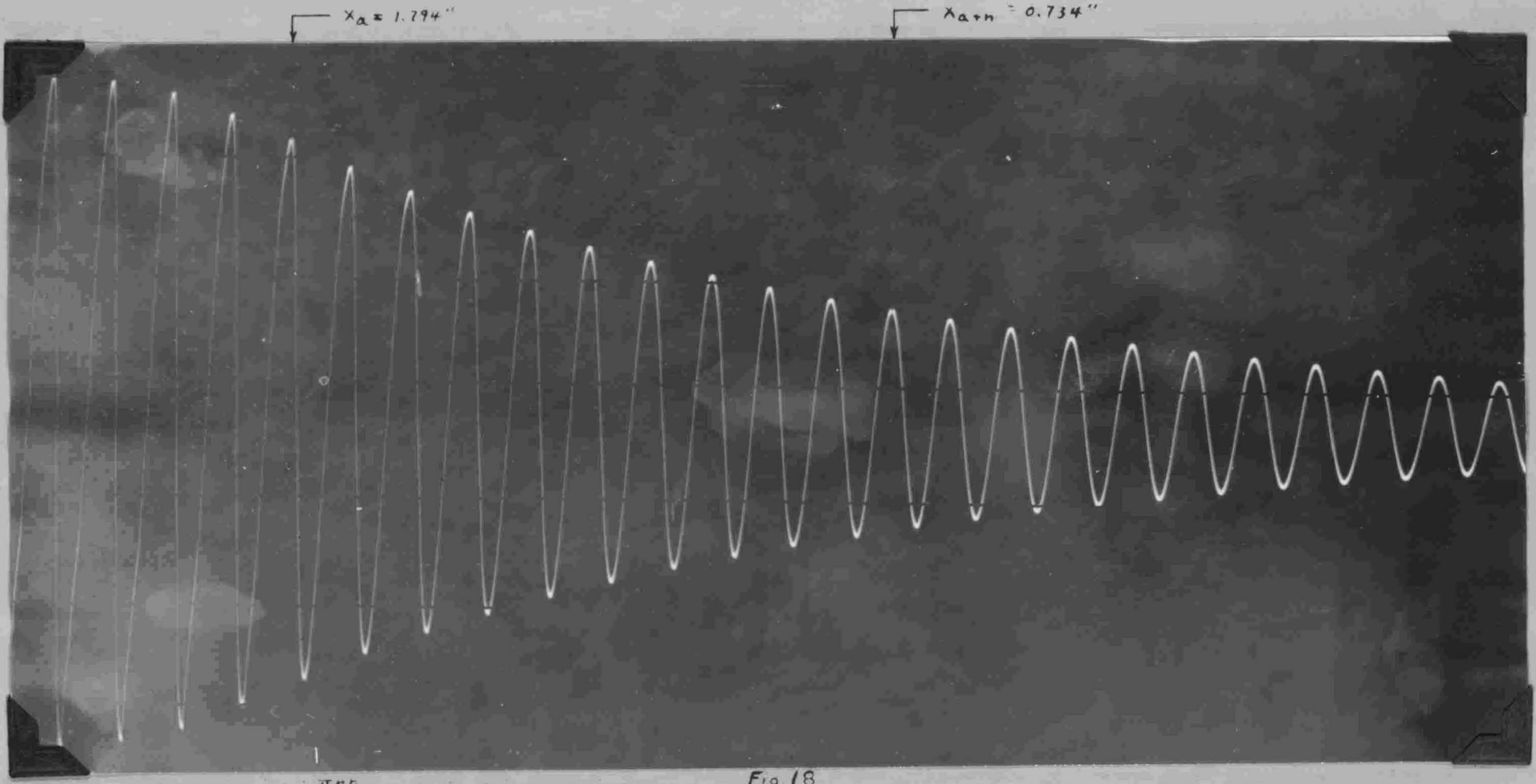

Fig 18

OSCILLOGRAM OF DIE-AWAY CHARACTERISTIC OF MAIN SYSTEM

$$x_{a+n} = x_a \epsilon^{-\frac{\pi n b}{m q}}$$

Where: x_a Max amplitude of a th cycle = 1.794"

x_{a+n} Max amplitude on (a+n)th cycle = 0.734"

n = Number of cycles between measurement points = 10

b - Damping Constant of system.

m = Mass of system (including mass of locked plunger = 4.426 lbs = .1377 slugs.

q = Damped natural frequency of system (with plunger locked) = 57.4 Cycles/sec = 3600 Radians/sec

Substituting and solving for b: $b = 1.41$ slugs/sec

But $b_c = 2 m \omega_n = 2 \times .1377 \times 3600 = 99.3$ Slugs/sec = Critical damping Constant.

$\therefore \frac{b}{b_c} = \frac{1.41}{99.3} \times 100 = 1.42$ %

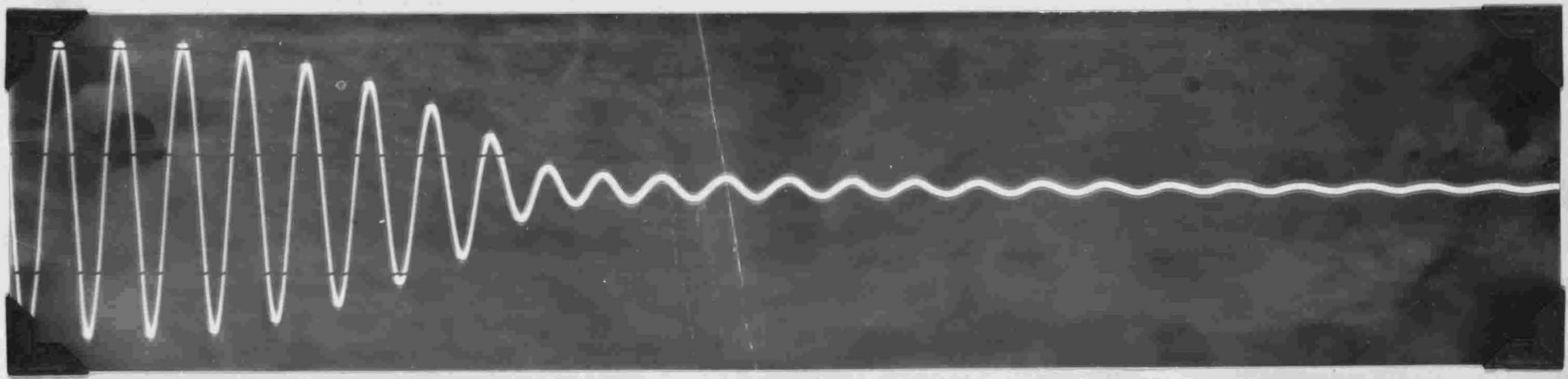

Fig. 19

Oscillogram showing effect of absorber on die-away characteristic using Navy symbol No. 3042 oil. Taken under condition of optimum tuning and $\omega = \Omega_n = 59.0$ cycles/sec.

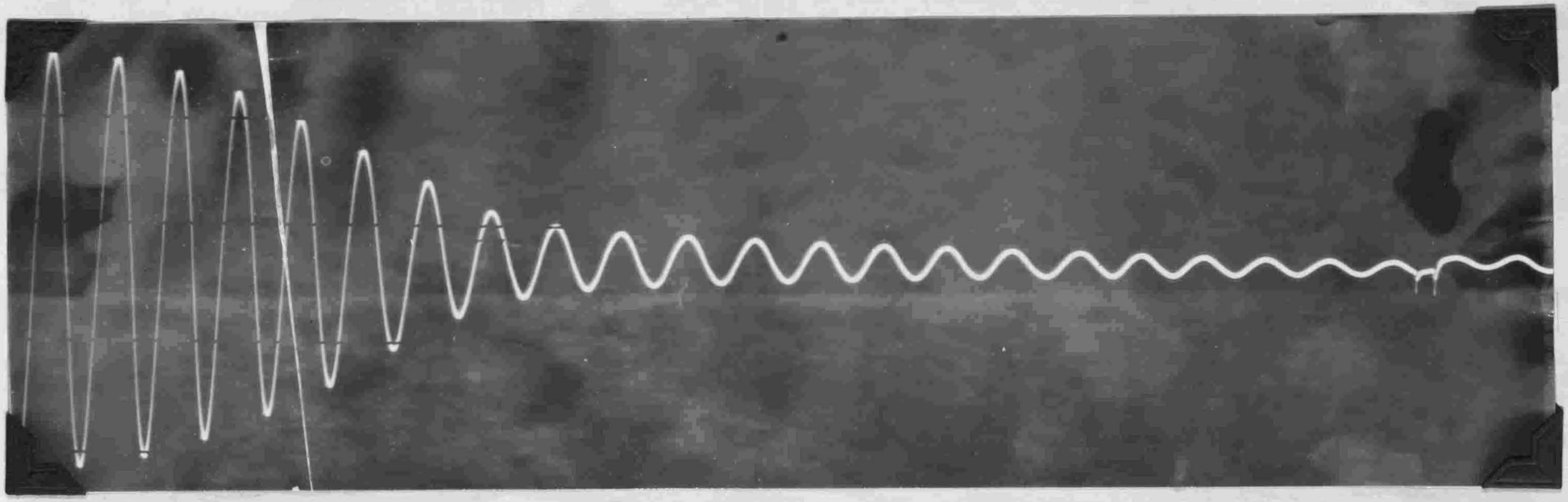

Fig. 20

Oscillogram showing effect of absorber on die-away characteristic using Navy symbol No. 2135 oil. Taken under condition of optimum tuning and $\omega = \Omega_n = 59.0$ cycles/sec.

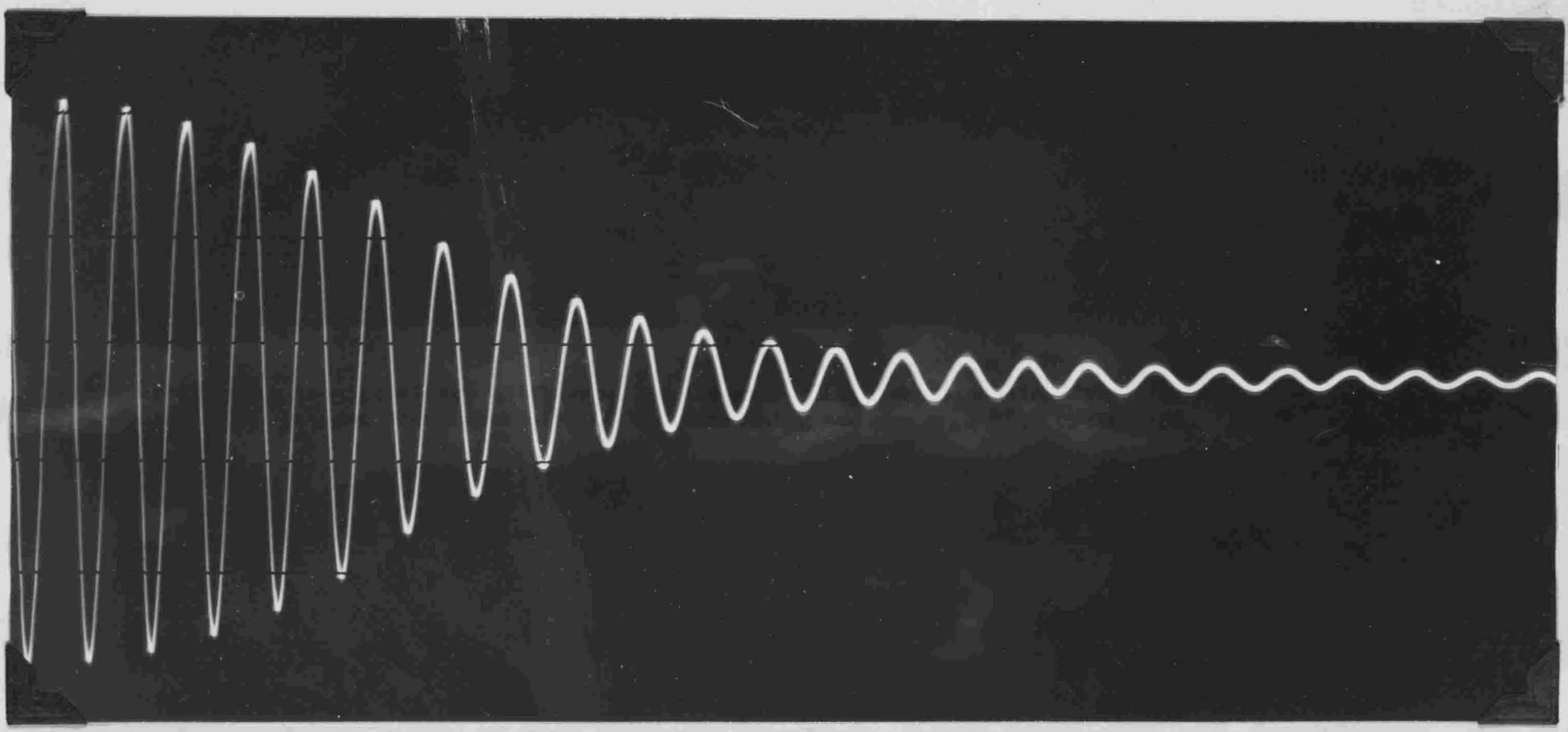

Fig. 21

Oscillogram showing effect of absorber on die-away characteristic using Navy symbol No. 1065 oil. Taken under condition of optimum tuning and $\omega = \Omega_n = 59.0$ cycles/sec.

CHAPTER V

DISCUSSION AND CONCLUSIONS

A remarkably close correlation between the theory and the experimental results is demonstrated by Figs. 15 and 16. The calculated curve for the infinite damping condition for both the constant and optimum tuning case practically coincides with the experimental curve.

In Fig. 16, a comparison of the calculated curves for a damping ratio, h, of 0.1, 0.2, and 0.3 with the experimental curves for Navy symbol number 3042, 2135, and 1065 oil, respectively, reveals the same general shape for corresponding damping conditions. Neglecting the main system damping constant, b, which is quite small, and substituting in equation (26) for the case of optimum tuning, it is found that the optimum damping ratio, h, is 0.140. Therefore, the calculated curve for $h = 0.1$ is underdamped and the curves for 0.2 and 0.3 are overdamped. By comparison with the experimental curves, it is estimated that the damping ratio, h, for oil #3042 is about 0.11; for oil #2135, about 0.19; and for oil #1065, about 0.32.

A comparison of the experimental curves for constant tuning, Fig. 15, with the corresponding curves for optimum tuning, Fig. 16, clearly shows the advantage, predicted by the theory, of optimum tuning. The desirability of optimum damping is clearly evident from Fig. 16.

In Chapter II, section 6, it was pointed out that there was no value of the driving frequency ratio, g, other than the trivial case of $g = 0$, which would make the amplitude ratio x_1/x_0, independent of damping unless the main system damping constant, b, was zero; in which case x_1/x_0 was independent of damping for two values of g, designated as g_1 and g_2, and all curves pass through two common points, designated as P and Q.

with abscissas g_1 and g_2, respectively. The absence of ~~a~~ definite P and Q points when b is not zero is illustrated by the theoretical curves of Fig. 16 which were computed for a b of about 1.4% of critical. The reader is refered to Den Hartog (3) for theoretical curves when b is zero.

Both the theoretical and the experimental curves demonstrate that the absorber serves no useful purpose in the frequency ratio range below about 0.88 and above about 1.06. In fact, the absorber is a detriment to best performance in these regions. Brock (2) suggests that the optimum procedure would be to use infinite damping until $g = g_1$, to use zero damping from $g = g_1$ to $g = g_2$, and to use infinite damping beyond $g = g_2$. In a practical case, this would necessatate cutting the absorber in (unlocking plunger) at some point below the resonant frequency of the system and cutting the absorber out (locking plunger) at some point above the resonant frequency. Such a procedure is hardly justified for the slight gain in performance which the curves of Figs. 15 and 16 indicate would be achieved. However, if an absorber is used in order to permit smooth acceleration through the resonant frequency range to an operating speed above the resonant frequency range, then it would be advantageous to cut the absorber out (lock plunger) after reaching the operating speed, therby slightly reducing the amplitude of vibration and saving unnecessary wear of the absorber.

The relative motion between the absorber plunger and cylinder results in a shearing action on the oil film in the clearance space and a dissipation of energy as heat. It would be expected that the temperature of the oil film would rise until a stabilized balance was reached between the heat energy generated in the oil film and that conducted away through the walls of the absorber and eventually dissipated to the atmosphere. That such a condition occures is demonstrated by the temperature rise curves of Fig. 17. However, the amount of temperature rise is surprisingly small, being in the order of 3 to 5 °F on the surface of the cylinder. It is interesting to note that of the three oils tested, the heavest oil caused the greatest temperature rise.

A point worthy of mention is that the oil film exibited no obserable tendency to break-down or vibrate-out of the clearance space even though the absorber was frequently operated continously for 4 to 6 hours.

The main system damping constant, b, as computed by equation (11) and based on the observed resonant amplitude of vibration is in close agreement with the value obtained by the application of the logarithmic decrement method to the oscillogram of the die-away characteristic. By applying equation (11) to the plunger-locked curve for the constant tuning case of Fig. 15, b was found to be 1.392% of the critical damping constant, b_c; a similar computation for the optimum tuning case gave a b of 1.396%; whereas, computations based on the die-away characteristic of Fig. 18 gave a value of b of 1.42%. The difference between the values is considerably less than a tenth of one percent (0.1%) and well within experimental accuracy.

The damping effect of the absorber is well demonstrated by the oscillograms shown in Figs. 19, 20, and 21. The oscillograms were taken under the conditions outlined in Chapter IV, section 12, and illustrate the effect of the absorber on the die-away characteristic of the main elastic system. Oil #3042, which as previously noted is close to the optimum damping condition, produced the most effective die-away damping action, causing the vibration to be reduced to a very small amount within 6 cycles of the power cut-off point. Oils 2135 and 1065 are progressively worse in this respect as would be expected from the results of Fig. 16. The rapidity of the die-away may be compared with the plunger-locked case of Fig. 18. It is also interesting to compare the amplitude of the waves (indicative of the amplitude of vibration) of Figs. 19, 20, and 21 under the steady state condition before the power cutt-off point. These oscillograms, however, are not comparable on an amplitude bases with Fig. 18 due to a different setting of the signal gain for this case. It will be observed that oil 3042 gives the minumum steady state amplitude, with oil 2135 and 1065 giving progressively higher amplitudes, as would be expected from the results of Fig. 16.

BIBLIOGRAPHY

1. Brock, J.E.: A Note on the Damped Vibration Absorber, Trans. A.S.M.E. (J. Applied Mech.), v14, Dec. 1946, p.A284.

2. Brock, J.E.: Theory of the Damped Dynamic Vibration Absorber for Inertial Disturbances, Trans. A.S.M.E. (J. Applied Mech.), v16 March 1949, p.86-92.

3. Den Hartog, J.P.: Mechanical Vibrations, 3rd. ed., McGraw-Hill, 1947.

4. Root, R.E.: Dynamics of Engine and Shaft, Wiley, 1932.

5. Wahl, A.M.: Mechanical Springs, Penton Publishing Co., 1944.